Environmental changes during the Cretaceous-Paleogene mass extinction and Paleocene-Eocene Thermal Maximum: Implications for the Anthropocene

Gerta Keller [a,*], Paula Mateo [h], Jahnavi Punekar [b], Hassan Khozyem [c], Brian Gertsch [i], Jorge Spangenberg [e], Andre Mbabi Bitchong [f,g], Thierry Adatte [d]

[a] Department of Geosciences, Princeton University, Princeton, NJ 08544, USA
[b] Indian Institute of Technology Bombay, Mumbai 400076, India
[c] Department of Geology, Faculty of Sciences, Aswan University, Aswan, Egypt
[d] Institute of Earth Sciences (ISTE), University of Lausanne, 1015 Lausanne, Switzerland
[e] Institute of Earth Surface Dynamics (IDYST), University of Lausanne, Switzerland, 1015 Lausanne, Switzerland
[f] Department of Earth Sciences, Faculty of Science, University of Yaounde 1, P.O. Box 812, Yaounde, Cameroon
[g] Department of Petroleum and Gas Exploration, Institute of Mines and Petroleum Industries, University of Maroua, P.O. Box 08, Kaele, Cameroon
[h] Division of Geological and Planetary Sciences, California Institute of Technology, Padadena, 91125, CA
[i] Swiss National Science Foundation (SNSF), Wildhainweg 3, P.O. Box, CH 3001 Berne, Switzerland

ARTICLE INFO

ABSTRACT

The Cretaceous-Paleogene boundary (KPB) mass extinction (~66.02 Ma) and the Paleocene-Eocene Thermal Maximum (PETM) (~55.8 Ma) are two remarkable climatic and faunal events in Earth's history that have implications for the current Anthropocene global warming and rapid diversity loss. Here we evaluate these two events at the stratotype localities in Tunisia and Egypt based on climate warming and environmental responses recorded in faunal and geochemical proxies. The KPB mass extinction is commonly attributed to the Chicxulub impact, but Deccan volcanism appears as a major culprit. New mercury analysis reveals that major Deccan eruptions accelerated during the last 10 ky and reached the tipping point leading up to the mass extinction. During the PETM, climate warmed rapidly by ~5 °C, which is mainly attributed to methane degassing from seafloor sediments during global warming linked to the North Atlantic Igneous Province (NAIP). Biological effects were transient, marked by temporary absence of most planktic foraminifera due to ocean acidification followed by the return of the pre-PETM fauna and diversification. In contrast, the current rapid rise in atmospheric CO_2 and climate warming are magnitudes faster than at the KPB or PETM events leading to predictions of a PETM-like response as best case scenario and rapidly approaching sixth mass extinction as worst-case scenario.

© 2017 International Association for Gondwana Research. Published by Elsevier B.V. All rights reserved.

1. Introduction

One of the greatest challenges to our planet is the looming Anthropocene mass extinction commonly attributed to human activity as the dominant influence on rapid climate warming and changing environments as a result of fossil fuel burning (IPCC 5th Assessment Report, 2013). This climate warming is commonly compared with the rapid short-term ~5 °C warming known as the Paleocene-Eocene Thermal Maximum (PETM) ~55.8 Ma. However, the PETM led to opposite results: major diversification in marine and terrestrial life and significant species extinctions only in deep-water benthic foraminifera. A better understanding of the impending Anthropocene catastrophe can be gained from the rapid warming and mass extinction culminating at the Cretaceous-Paleogene boundary (KPB also known as KPgB or KTB). In this study we examine both the PETM and KPB events to gain insights into potential Anthropocene scenarios.

The PETM event (55.8 ± 0.2 Ma) lasted ~170 ky and is commonly attributed to North Atlantic Igneous Province (NAIP) volcanism and methane degassing of seafloor sediments (e.g., Dickens et al., 1995; Dickens, 2000; Westerhold et al., 2009; Charles et al., 2011; Wieczorek et al., 2013; Gutjahr et al., 2017). The resulting global negative $\delta^{13}C$ excursion of 2–6‰ and rapid warming of 4.5–5 °C from tropical to high latitudes was accompanied by ocean acidification and shoaling of the carbonate compensation depth (CCD) by ~2000 m (e.g., Kennett and Stott, 1991; Sluijs et al., 2006; Zachos et al., 2003, 2005, 2006; Weijers et al., 2007; McInerney and Wing, 2011; Coccioni et al., 2012; Gutjahr et al., 2017). In the marine realm

planktic foraminifera and calcareous nannoplankton, which form the essential food chain in the oceans, temporarily disappeared but returned and diversified after the PETM (Lu and Keller, 1993, 1995a, 1995b; Kelly et al., 1996, 1998; Luciani et al., 2007, 2016). Only benthic foraminifera suffered significant extinctions and these were restricted to bathyal depths where an estimated 37% species went extinct (Alegret and Ortiz, 2006). No other groups in marine or terrestrial realms suffered significant extinctions. On land tropical and subtropical forests spread into higher latitudes during the PETM (Sluijs et al., 2006) and most animals reduced in size and abundance (Smith et al., 2009). Shortly after the PETM mammals migrated, thrived and diversified (Smith et al., 2009).

The KPB mass extinction (66.02 Ma) was marked by a negative 2–3‰ $\delta^{13}C$ shift in surface but not deep waters, leading to an inverse surface-to-deep $\delta^{13}C$ gradient generally attributed to reduced primary productivity and weakening of the marine biological carbon pump (e.g., Zachos et al., 1989; Kump, 1991, 2003). Rapid climate warming during the last 350 ky of the Maastrichtian, prior to the KPB, and cooling during the first 500 ky of the early Paleocene are linked to Deccan volcanic eruptions (review Punekar et al., 2014) About 50–75% of all terrestrial and marine taxa went extinct. In the oceans, extinctions affected the base of the food chain most severely causing major extinctions in calcareous nannoplankton and near total extinction (99%) of marine planktic foraminifera (e.g., Keller, 1988a, 2001; MacLeod et al., 1997; Molina et al., 1998; Keller et al., 2002; Luciani, 2002), but no significant extinctions in benthic foraminifera (review in Culver, 2003). The extinction of non-avian dinosaurs is the most famous example of the KPB mass extinction on land while many mammals survived undergoing an explosive radiation during the Paleogene (review in Feduccia, 2014; Wilson, 2014). Macrofloral diversity also decreased during the late Maastrichtian warming and across the mass extinction horizon (e.g., Wilf et al., 2003; Wilf and Johnson, 2004).

Both PETM and KPB events thus recorded extreme and rapid climate changes but with nearly opposite effects on marine and terrestrial life – rapid evolutionary diversification following the PETM event with extinctions restricted to deep water benthic foraminifera but near total mass extinction in planktic foraminifera at the KPB. Understanding when rapid climate change furthers evolutionary diversification and when it leads to extinctions is critical to assessing the risk of current climate warming for marine and terrestrial populations including humans in the coming decades. This study explores the potential reasons for the differing biotic responses associated with rapid climate warming during the PETM and KPB events and compares these with the current rapid climate warming and biotic response of the Anthropocene. We hypothesize that the biotic response mainly depends on the rate and tempo of greenhouse gas emissions into the atmosphere and that extinctions are inevitable once the tipping point or critical threshold is reached, which marks the onset of irreversible climate change from which even small perturbations can result in runaway effects.

For this study we chose the globally recognized most complete sections for the KPB and PETM events. For the KPB these are the Global Stratotype Section and Point (GSSP) at El Kef and the auxiliary stratotype at Elles (Molina et al., 2009) 56 km southeast of the city of El Kef, Tunisia, and for the PETM, the global GSSP at the Dababiya quarry in Egypt (Figs. 1, 2). We focus on four topics: 1) planktic and benthic species population changes in foraminifera, the groups most strongly affected by both events; 2) evidence linking mass extinctions and faunal turnovers to climate change and ocean acidification; 3) evidence linking these faunal events directly to volcanism; and 4) comparison of KPB and PETM with the Anthropocene and potential sixth mass extinction. Analyses are based on benthic and planktic foraminifera, carbon and oxygen stable isotopes, mineralogy, and mercury (Hg) anomalies. (A description of methods, materials and locations and of the environmental proxies is given in Supplementary materials S1; data tables are given in Supplementary materials S2.)

2. KPB mass extinction: El Kef and Elles

2.1. KPB-defining criteria

The KPB is one of the easiest period boundaries to identify, whether based on lithological changes in the field (Fig. 3), geochemical analysis in the laboratory, or fossil content. The El Kef section was officially designated in 1989 as the Global Stratotype Section and Point (GSSP) and Elles (discovered in the late 1990s) designated as auxiliary stratotype (Molina et al., 2009). The five KPB defining and marker criteria are: (1) mass extinction in planktic foraminifera, (2) evolution of first Danian species, (3) KPB clay and red layer, (4) iridium (Ir) anomaly and (5) $\delta^{13}C$ negative shift. These KPB criteria have proven globally applicable and independently verifiable in over 300 KPB sequences worldwide (Cowie et al., 1989; Keller et al., 1995; Remane et al., 1999). Since planktic foraminifera are the only marine microfossil group that suffered near total extinction, they have remained the most reliable KPB-defining criteria. All other KPB markers, such as the clay and red layers, Ir anomaly and $\delta^{13}C$ shift, are not unique signals in the geological record and therefore cannot define the KPB in the absence of unique biomarkers (review in Keller, 2011).

However, proponents of the Chicxulub impact as sole cause for the mass extinction eliminated the five KPB identifying criteria in favor of just the "*Ir anomaly associated with a major extinction horizon*" (Gradstein et al., 2004, ICS website on GSSPs). Based on these two criteria and the assumption that the Ir anomaly is the result of the Chicxulub impact, Molina et al. (2006, p. 263) concluded that "*in this way the KPB is marked exactly by the moment of the meteorite impact*" and that "*This definition solves problems of correlation in the Yucatan peninsula (Mexico) and its surroundings.*" Far from solving "problems of correlation", this new definition has only introduced circular reasoning to support the hypothesis that the Chicxulub impact is precisely KPB in age, thus ignoring contrary evidence (Keller, 2011, Supplementary materials S3). Fortunately, the El Kef and Elles KPB sections remain identified by the original five criteria that are the most reliable KPB markers.

2.2. Biostratigraphy: planktic foraminifera

Zone definitions are based on Keller et al. (1995, 2002) and include: zone CF2 (last appearance (LA) of *Gansserina gansseri* near the base of magnetochron C29r to first appearance (FA) of *Plummerita hantkeninoides*), zone CF1 (range of *Plummerita hantkeninoides*, extinct at the KPB), zone P0 (from the KPB to FA of *Parvularugoglobigerina eugubina*), zone P1a(1) (FA of *P. eugubina* to FAs of *Parasubbotina pseudobulloides* and/or *Subbotina triloculinoides*), and zone P1a(2) (LAs of *P. eugubina* and *P. longiapertura*) correlative with the top of magnetochron C29r (Fig. 4). Thus, zones CF2 through P1a(2) correlate with magnetochron C29r (Li and Keller, 1998; Pardo et al., 1996). The time interval presented in this study for El Kef spans from the latest Maastrichtian zone CF1 through the early Danian zones P0, P1a(1), P1a(2) and lower part of P1b and for Elles from the upper part of zone CF1 to zone P1a(1).

Recent U-Pb zircon dating of Deccan Traps yielded a duration of ~750 ky for C29r (Schoene et al., 2015) with 250 ky equivalent to zones CF1-CF2 below the KPB and 500 ky equivalent to P0, P1a(1) and P1a(2) above the KPB. The late Maastrichtian intervals used in this study at El Kef and Elles span the last ~68 ky and 70 ky below the KPB and first ~500 ky and ~150 ky of the early Danian, respectively, plus an unknown age interval of zone P1b in C29n (Fig. 4).

2.3. Extinctions and survivals

The mass extinction at El Kef is shown in Fig. 4 based on species ranges and morphologies of the different planktic foraminiferal groups. The largest most specialized and highly ornamented taxa, known as K-strategists (Fig. 4 #1–10), generally lived below the surface in tropical
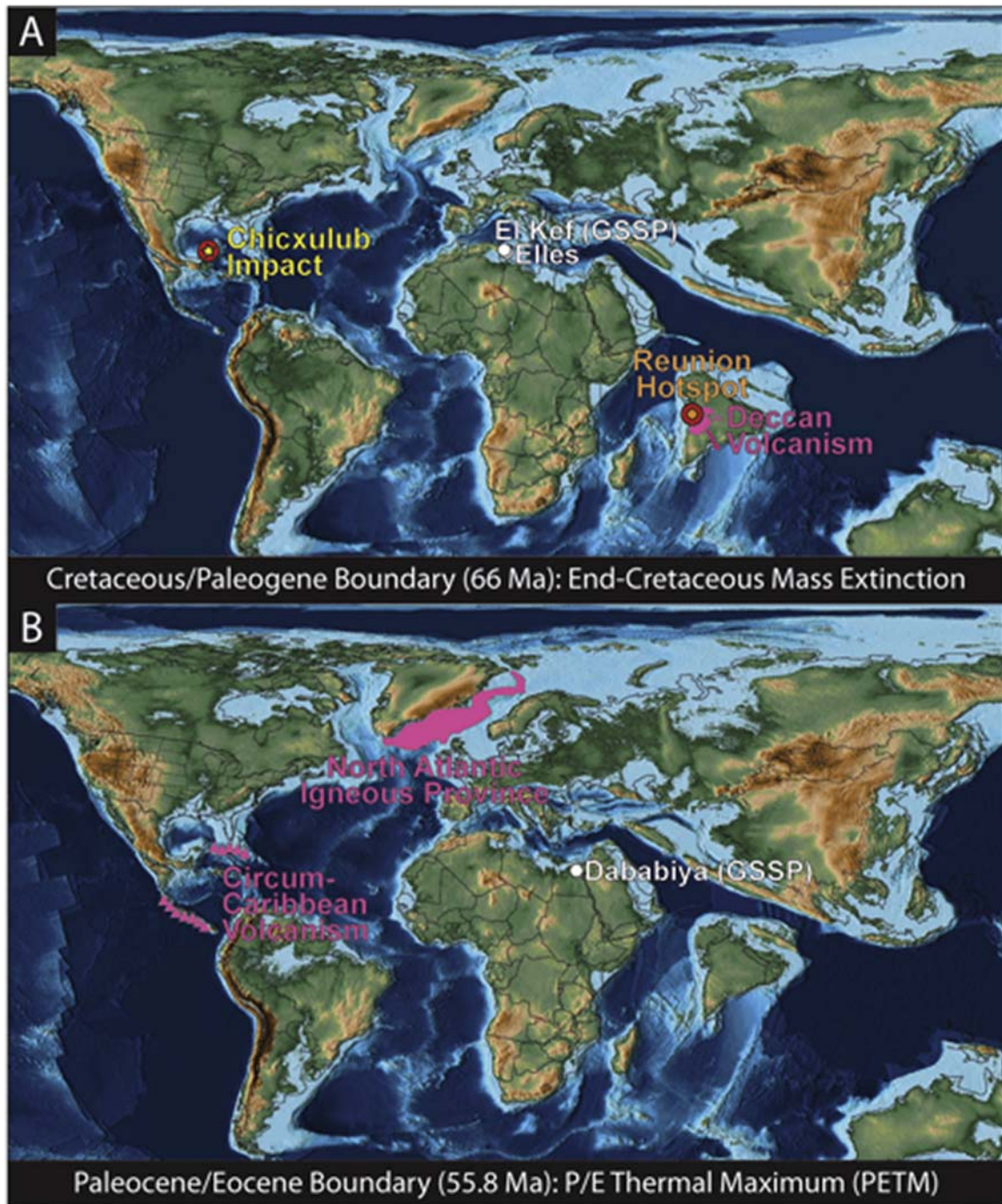
Fig. 1. (A) Paleogeography at the KPB (66.02 Ma) and paleolocations of El Kef and Elles sections, Reunion hotspot, Deccan volcanism and Chicxulub impact site. (B) Paleogeography at the PEB (55.8 Ma) and paleolocations of the Dababiya section, North Atlantic Igneous Province and circum-Caribbean volcanism. Paleomaps from Scotese (2013a, 2013b).

and subtropical waters, utilized specialized food sources, had few off-spring and lived longer (Begon et al., 1996, 1998). They suffered reduced population abundances and species dwarfing during the late Maastrichtian climate warming linked to Deccan volcanism in C29r, zones CF1-CF2 (Li and Keller, 1998; Olsson et al., 2001; Abramovich et al., 2003, 2010; Keller and Abramovich, 2009; Punekar et al., 2014; Thibault et al., 2016; Thibault and Husson, 2016).

Quantitative species abundances at El Kef show that during this global warming complex larger specialized species decreased in abundance and diversity (Fig. 5) as also observed at Elles and worldwide (Abramovich and Keller, 2002; Punekar et al., 2014; Keller et al., 2016). Among this group, the robust globotruncanids (16 species) are

generally rare with combined abundance of 6–13%, which demonstrates the severe toll climate warming and related stresses (e.g., ocean acidification, high nutrient influx from Deccan volcanism and terrestrial runoff due to increased humidity) exerted on marine plankton leaving them prone to extinction.

A small group of species (about 1/3 of planktic foraminiferal assemblages) survived relatively well during the pre-KPB C29r climate warming (zone CF1, Figs. 4, 5). These were relatively small species with simple biserial and trochospiral morphologies, with little shell ornamentation. They were ecologically more tolerant, r-strategists that thrived in varied environments from low to high latitudes, utilized diverse food sources, had short life spans and reproduced rapidly with
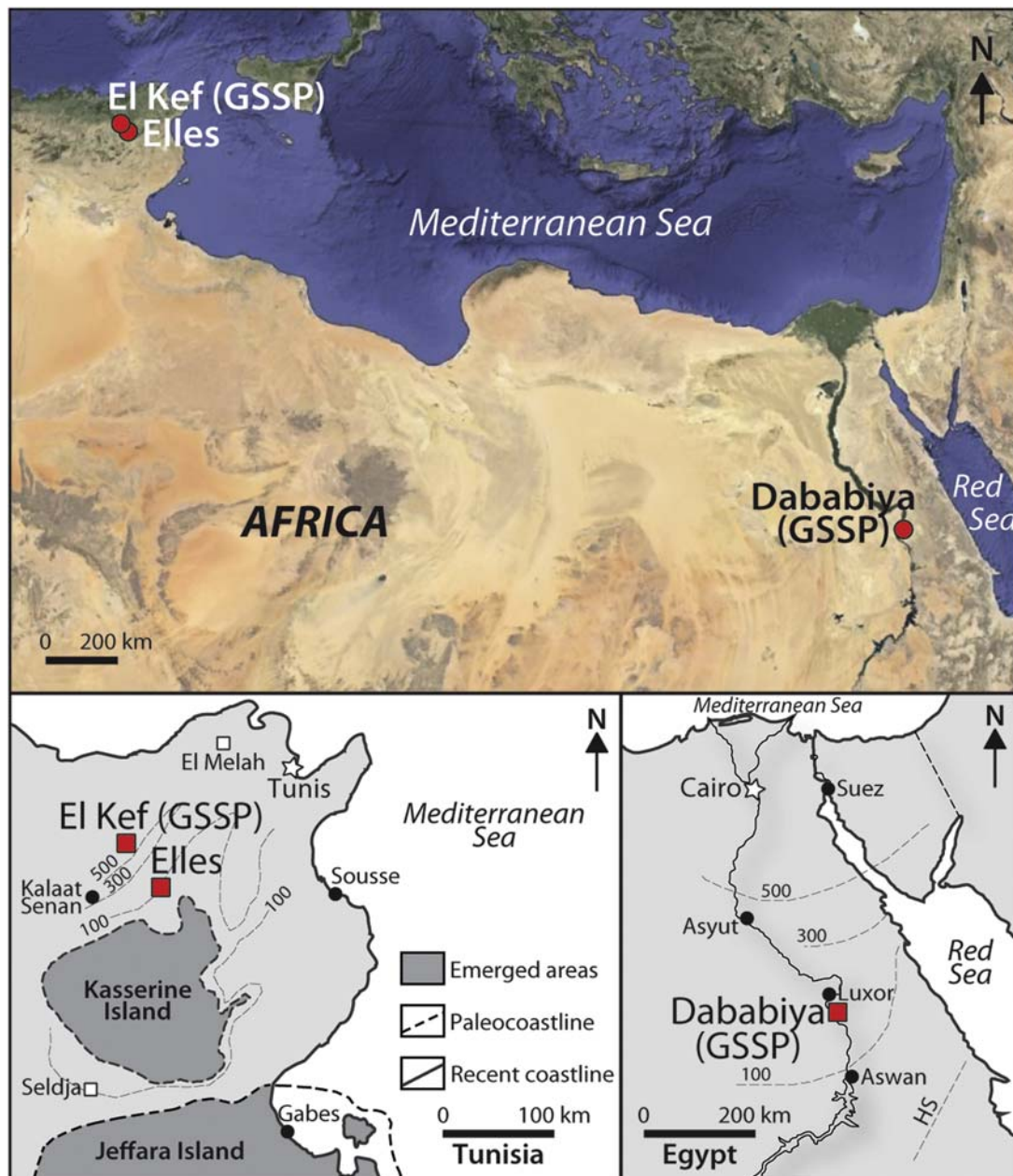
Fig. 2. Locations of the Cretaceous-Paleogene boundary (KPB) GSSP El Kef and Elles, Tunisia, and the Paleocene-Eocene boundary (PEB) GSSP at Dababiya, Egypt.

many offspring (review in Keller and Abramovich, 2009). This group had high survival potential but just one species survived long-term – the disaster opportunist *Guembelitria cretacea.*

There is general agreement that between 8 and 16 smaller species survived for about 50–150 ky into the early Danian (Figs. 4, 5) but survivorship is difficult to ascertain for most species because reworked Cretaceous species are common above the KPB. This is mainly due to the early Danian global cooling, lower sea level and erosion that frequently resulted in hiatuses eroding the underlying KPB interval and latest Maastrichtian particularly in shallow water environments (Keller et al., 2013, 2016; Mateo et al., 2017). Clues to survivorship include consistent presence in Danian sediments, good preservation, generally dwarfed specimens and Danian isotope values. Only *Heterohelix globulosa, H. planata, Paraspiroplecta navarroensis, Pseudoguembelina costulata, Guembelitria cretacea, Hedbergella monmouthensis, H. holmdelensis, Globigerinelloides asper* and *G. yaucoensis* are proven mass extinction survivors to date (e.g., Barrera and Keller, 1990; Pardo

and Keller, 2008; Ashckenazi-Polivoda et al., 2011). Other species are also consistently present well into the early Danian but have yet to be conclusively determined as survivors (e.g., *Pseudoguembelina costellifera, P. kempensis, Globigerinelloides subcarinatus*; Figs. 4–6).

Among the survivors, four biserial species (*P. costulata, H. globulosa, H. planata, P. navarroensis*), at least three trochospiral species (*Hedbergella monmouthensis, H. holmdelensis, Globigerinelloides yaucoensis*), and one triserial species (*G. cretacea*), are known to tolerate low oxygen conditions. These dominate late Maastrichtian assemblages and range well into the early Danian with reduced to sporadic presence (Figs. 4–6) (Pardo and Keller, 2008; Ashckenazi-Polivoda et al., 2011). But they also suffered beginning in the latest Maastrichtian (upper zone CF1) and into the early Danian as evident by species dwarfing, deformed chambers and reduced population abundances (Fig. 6) (review in Keller and Abramovich, 2009).

The KPB mass extinction has just one long-term survivor, *G. cretacea*, which is known as a disaster opportunist. This species thrived during

Fig. 3. (A) The KPB event at Elles, Tunisia, is well exposed across the hillside marked by a lithological change from gray shale of the Maastrichtian to dark gray clay of the early Danian weathered to a light brownish color. (B) A 1–2 cm thick rusty "red layer" at the base of the KPB clay layer contains maximum Ir concentrations and marks the mass extinction. (C) A blow-up of this red layer shows the sharp contact with the Maastrichtian marl below and dark Danian clay of zone P0 above. (For interpretation of the references to color in this figure legend, the reader is referred to the web version of this article.)

maximum stress conditions and dominated faunal assemblages of the latest Maastrichtian and early Danian (>90%) at El Kef and Elles (Figs. 5, 6) (Pardo and Keller, 2008; Punekar et al., 2014). *Guembelitria cretacea* was the smallest planktic foraminifer (63–100 μm) and responded to highest-stress conditions by dwarfing (size reduction to 38–63 μm), irregular deformed chambers (Coccioni and Luciani, 2006), and less frequently
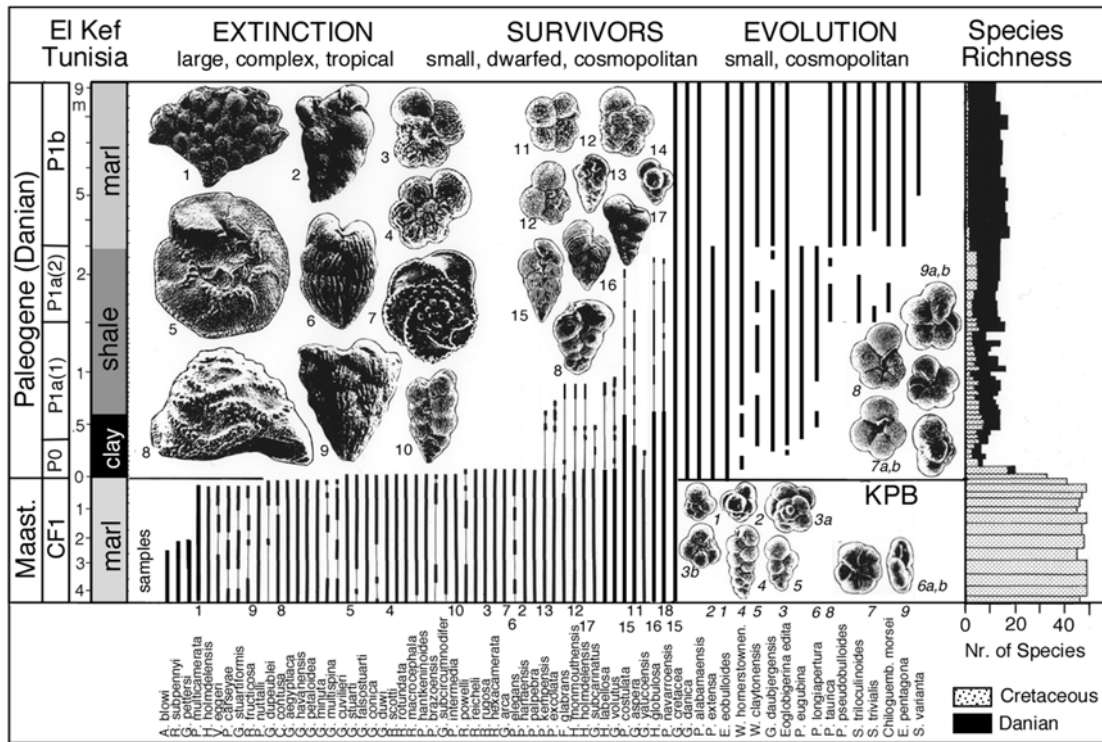

Fig. 4. KPB extinction pattern at El Kef, Tunisia, shows all large tropical to subtropical species extinct at or near the KPB (2/3 of all species, SEM illustrations 1–10, numbers keyed to species), the short-term survivorship of small ecologically more tolerant species (1/3 of the species, SEMs 11–18) including a single long-term survivor (*Guembelitria cretacea*, SEM 14). Early Danian evolution begins within a few thousand years of the mass extinction but diversity remains low and species small (SEMs 1–9) marking high-stress conditions over ~500 ky of the earliest Danian. SEM illustrations are shown in relative species sizes in the assemblages. Faunal data updated from Keller (1988a).
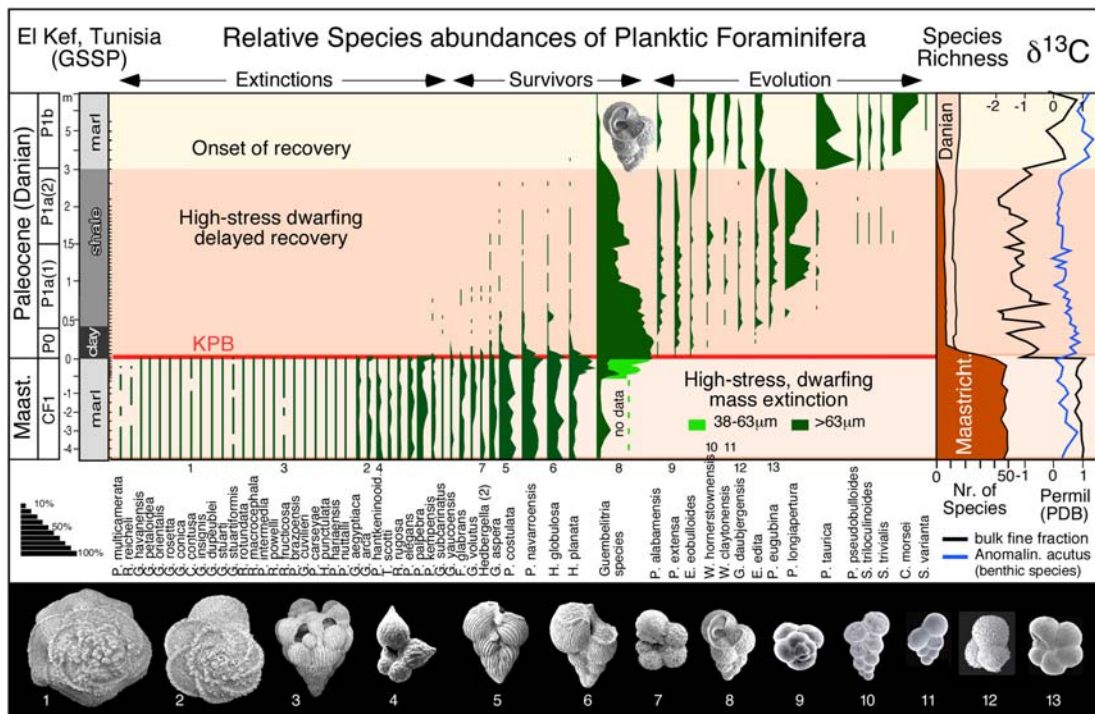
Fig. 5. El Kef, Tunisia, relative abundances of planktic foraminifera across the KPB (>63 µm size fraction for all species except 38–63 µm for *Guembelitria*) with SEM illustrations of marker species (numbers keyed to species names and abundance data). Carbon stable isotopes of bulk rock and benthic species *Anomalinoides acutus* across the KPB transition. Note the abrupt diversity change that marks the KPB mass extinction and the δ13C negative shift that signals the collapse of primary productivity. Faunal data from Keller (1988a, updated), isotope data from Keller and Lindinger (1989).

gigantism (Keller, 2014). During optimal environmental conditions, this disaster opportunist disappeared from open marine assemblages but survived in high-stress near-shore refugia.

2.4. Species dwarfing

Species dwarfing, also known as the Lilliput effect, marks morphologic and intraspecies size reductions in response to environmental stresses commonly associated with, but not restricted to, the aftermath of mass extinctions (Keller and Abramovich, 2009). In addition to planktic foraminifera across the KPB mass extinction, the Lilliput effect has been observed in many groups, including ostracods, mollusks and bivalves, of the Permo-Triassic mass extinction (Payne, 2005; Twitchett, 2007; Chu et al., 2015), shelly faunas and microbial carbonates preceding the end-Devonian mass extinction (Whalen et al., 2002; Bosetti et al., 2010), crinoids of the end-Ordovician mass extinction (Borths and Ausich, 2011) and graptolites of the upper Silurian (Urbanek, 1993). This suggests a universal biotic response to environmental stress, regardless of cause, timing or nature of organisms.

High-stress environments are associated with rapid climate change, mesotrophic or restricted basins, shallow marginal settings and volcanically active regions. For example, Large Igneous Province (LIP) volcanism is currently associated with four of the five Phanerozoic mass extinctions, whereas Hg anomalies, a proxy for volcanism, are reported from all five (da Silva et al., 2009; Grasby et al., 2013; Percival et al., 2015; Thibodeau et al., 2016; Font et al., 2016; Gong et al., 2017). Second order volcanic events (e.g., Ninetyeast Ridge and Andean volcanism) are at least in part related to the early late Maastrichtian faunal turnover (Keller, 2003; Keller et al., 2007; Mateo et al., 2017).

Among planktic foraminifera the sequence of responses to increasingly high environmental stress developed in 5 stages that form a stress continuum from optimum open marine conditions to increasingly stressful environments associated with rapid climate warming and volcanic activity leading to catastrophe (Fig. 7). The five stages of this stress continuum include: (1) elimination of large specialized species (K-strategists), (2) intraspecies dwarfing, (3) dominance of low oxygen tolerant small heterohelicids (r-strategists), (4) decline of heterohelicids and (5) dominance of disaster opportunist *Guembelitria* species (Keller and Abramovich, 2009).

This sequence of stress-induced biotic events is demonstrated at El Kef and Elles, as well as in all continuous KPB sequences worldwide (Pardo and Keller, 2008; Keller and Abramovich, 2009). Stages 1–2 are evident by the dramatic reduction in large K-strategist species populations and dwarfing of survivors, which was first linked to global warming caused by Deccan volcanism in magnetochron C29r at South Atlantic DSDP Site 525A (Abramovich and Keller, 2003). Stage 3 marks the rising dominance of r-strategists, followed by dwarfing in stage 4 and declining populations. Stage 5 marks maximum stress resulting in decreased populations of r-strategists and dominance of the disaster opportunist *Guembelitria*.

Fig. 6 shows the effects of species dwarfing across the KPB transition based on >63 µm and 38–63 µm size fractions at Elles. In the >63 µm size fraction below the KPB, the same four biserial taxa dominate the assemblage as at El Kef and *Guembelitria cretacea* is rare (Fig. 6A). After the mass extinction, *G. cretacea* dominates (>95%) but the interval between 7 cm to 80 cm above the KPB is barren in the >63 µm size fraction with species abruptly reappearing above (Fig. 6A).

Analysis of the smaller size fraction (38–63 µm) reveals the missing fauna as dwarfed due to increased stress (Fig. 6B). The most notable difference is the dominance of dwarfed disaster opportunist *G. cretacea* and low oxygen tolerant *P. navarroensis* and *H. planata*. Dwarfed *Guembelitria* populations up to 90% of the total foraminiferal assemblages are frequently observed below the KPB in shallow shelf to open marine and in volcanically stressed environments (review in Pardo and Keller, 2008). Similar *Guembelitria* blooms dominated (~90%) after the KPB mass extinction, although they are generally not dwarfed. This suggests that environmental stress was higher before the mass extinction than in its aftermath.
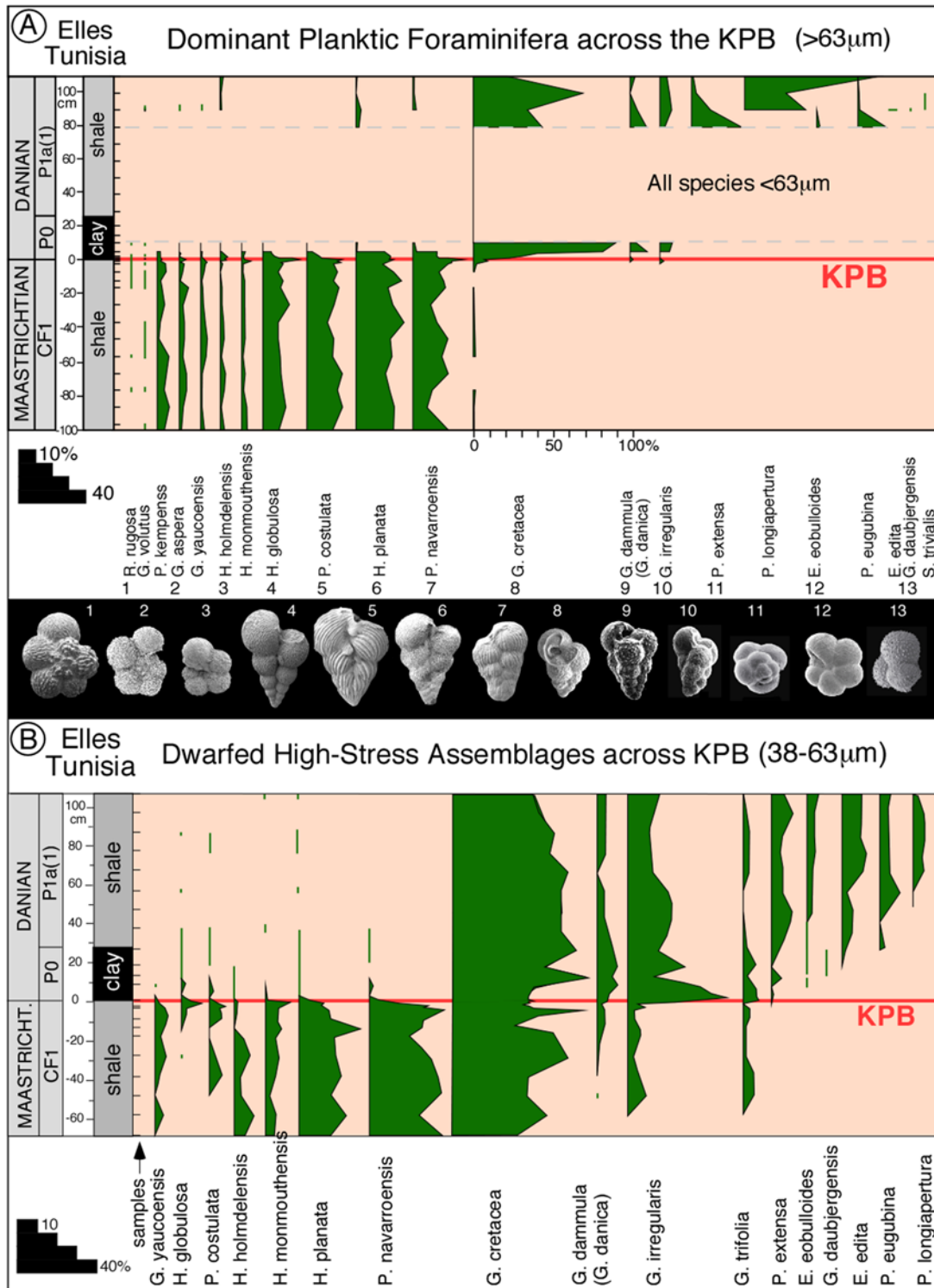
Fig. 6. (A) Relative abundances of planktic foraminifera (>63 μm) across the KPB at Elles, Tunisia, reveal low diversity assemblages dominated by small biserial species, but not *Guembelitria*, during the climate warming of the latest Maastrichtian and an interval of the early Danian. (B) Relative abundances of planktic foraminifera in the smaller (38–63 μm) size fraction reveals abundant dwarfed species in the earliest Danian as well as peak abundances (40%) during the latest Maastrichtian preceding the mass extinction. This indicates that dwarfing of the disaster opportunist *Guembelitria* is a response to extreme environmental stress. SEM illustrations (numbers keyed to species names) are shown in relative species sizes in the assemblages. Faunal data from Keller et al. (2002).

2.5. Evolution and delayed recovery

Evolution of new species began in zone P0 immediately after the mass extinction (Fig. 8). The first new species were very small (38–63 μm), unornamented, with simple globular chamber arrangements in biserial, triserial and trochospiral morphologies (Figs. 4–6). Low diversity assemblages of 10 to 15 species with slightly larger (63–100 μm) morphologies persisted for the first 500 ky (zones P1a(1)–P1a(2)) after the mass extinction, marking a long crisis interval. Cretaceous survivor species gradually disappeared in zone P1a(1) (Fig. 8). Dwarfing,
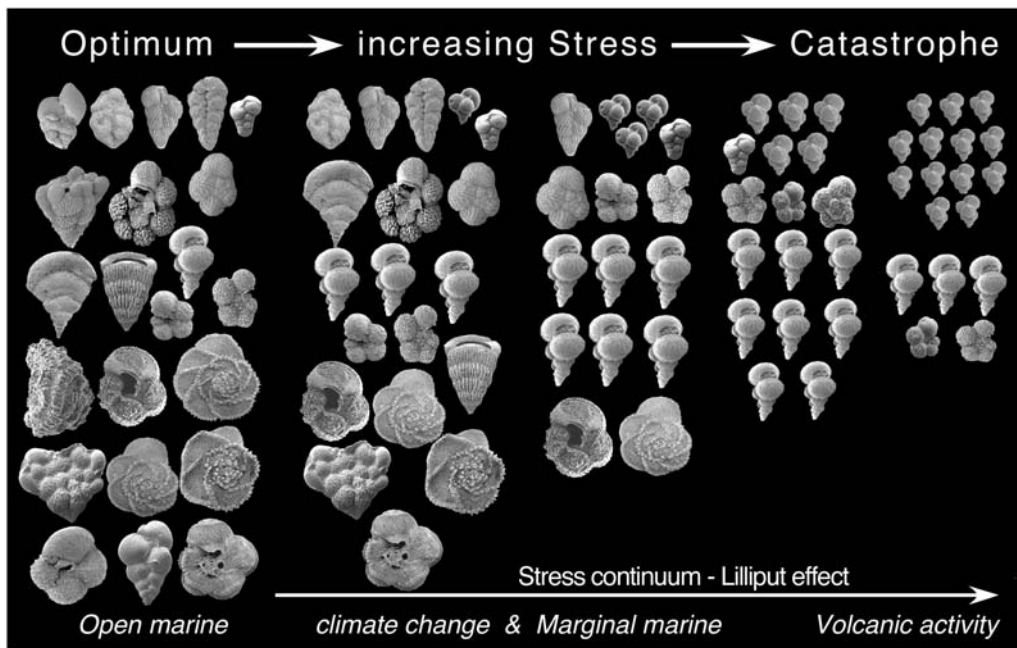
Fig. 7. Effects of increasing environmental stress upon planktic foraminiferal assemblages from optimum to catastrophe conditions. Note the successive elimination of large, specialized k-strategy species during climate warming, particularly in restricted basins and marginal marine environments, and the survival of small r-strategy species commonly associated with volcanic activity. Disaster opportunists flood the environment during catastrophes. Modified from Keller and Abramovich (2009).

slow evolution, simple small species morphology and gradual disappearance of dwarfed survivor species during the early Danian mark continued high-stress environments dominated by the disaster opportunist *Guembelitria* and the new crisis opportunists *Parvularugoglobigerina eugubina* and *P. longiapertura* (Figs. 5, 6).

A clue to the nature of this crisis interval is seen in the negative 2–3‰ δ^{13}C excursion at the KPB that represents a sudden drop in primary marine productivity at the mass extinction horizon (Fig. 5). During the early Danian, planktic δ^{13}C values at El Kef and Elles remained 1–2‰ below benthic values for the first ~500 ky correlative with the delayed
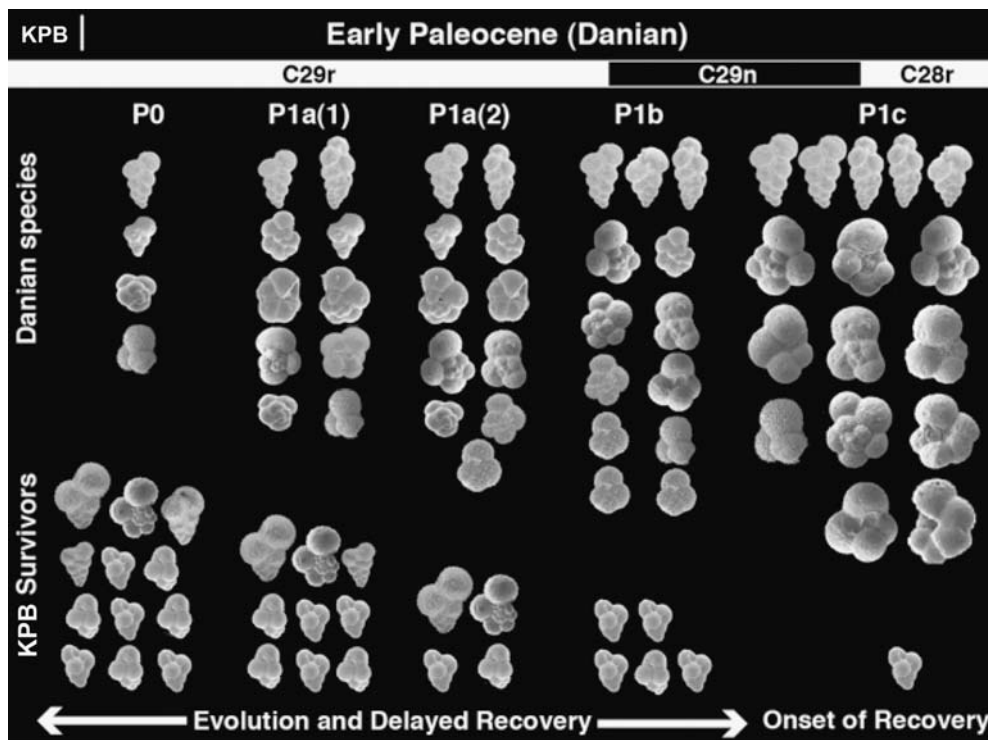

Fig. 8. Early Danian evolution and decline in Cretaceous survivor species illustrate high-stress environments. Small dwarfed species and low diversity mark delayed marine recovery in magnetochron C29r from zones P0 through P1a(2) correlative with decreasing abundance and gradual extinction of dwarfed survivor species. The last phase of Deccan volcanism began near the zone P1a/P1b boundary (C29r/C29n) and marks the extinction of two dominant zone P1a index species (*Parvularugoglobigerina eugubina*, *P. longiapertura*). Marine recovery begins after this last volcanic phase and is marked by higher diversity and increasing species sizes. Note the number of the same specimens in each column indicates relative abundance. From Punekar et al. (2014).

recovery in marine plankton (Keller and Lindinger, 1989; Stüben et al., 2003). This interval is followed by the rapid positive 2‰ δ^{13}C excursion at the P1a(2)/P1b zone boundary (C29r/C29n) that signals the onset of recovery coincident with the end of the main phase of Deccan volcanism (Fig. 5). Thus the delayed recovery appears to be due to continued volcanic eruptions. For marine plankton, the δ^{13}C recovery lead to a major re-organization, including the near disappearance of the disaster opportunist *Guembelitria* (Fig. 5), extinction of the dominant crisis interval taxa (*P. eugubina*, *P. longiapertura*, *P. extensa*), dominance of *Praemurica taurica* and small biserial low oxygen tolerant species (*Chiloguembelina morsei*, *Woodringina hornerstownensis*, *W. claytonensis*), increased diversity and gradual appearance of larger morphotypes particularly in zone P1c (Fig. 8).

2.6. Benthic foraminifera

There is no mass extinction in benthic foraminifera across the KPB globally but they suffered a severe and prolonged faunal turnover (Fig. 9). At El Kef, 42% (21 species) of 50 calcareous benthic species identified disappeared at the KPB and remained absent through the early Danian zone P1a—P1b interval analyzed (>500 ky) (Keller, 1988b). During the early Danian P0-P1a high-stress interval, 16% (8 species) temporarily disappeared, 30% (15 species) ranged through with *Anomalinoides acutus* dominant in the high-stress P1a interval and 12% (6 species) appeared in the early Danian. Correlative with this faunal turnover is the drop in CaCO₃ from ~50% (pre-KPB) to <10% (post-KPB) in the sediments, high terrestrial organic influx (due to enhanced weathering) and low oxygen in the water column and seafloor sediments (Keller and Lindinger, 1989). These high nutrient conditions favored epifaunal assemblages dominated by *A. acutus* scavenging food on the seafloor. Infaunal assemblages largely disappeared returning with increased oxygen in sediments in zone P1b (Fig. 9). Speijer and Van der Zwaan (1996) also analyzed El Kef benthic foraminifera. Their faunal turnover results slightly differ from Keller (1988b) with the main difference

being the larger number of disappearing and temporarily absent species, which is largely due to their inclusion of agglutinated and non-specified genera groupings.

How representative is the El Kef benthic faunal turnover pattern on a global basis? Culver (2003, p. 214) reviewed published reports across latitudes and palaeodepths and concluded: "*if the percentage data are taken at face value and averaged for shallow, intermediate and deep water, the results come out as follows: shallow, 40 % disappear; intermediate, 35 % maximum, 29 % minimum disappear; deep, 29 % maximum, 19 % minimum disappear.*" Note that "disappear" means that most or all of these taxa returned after the stress event in the aftermath of the KPB mass extinction. Although these data are incomplete and percentage values may have large errors, a major environmental change is evident on the seafloor across latitudes and palaeodepths but no mass extinction is recorded.

3. Environmental proxies: KPB

During the late Maastrichtian, rapid and extreme climate warming, interrupted by short cool events, began in the lower half of zone CF2, co-incident with the onset of major Deccan volcanic eruptions near the base of C29r about 350 ky prior to the mass extinction (Li and Keller, 1998; Punekar et al., 2014; Thibault et al., 2016). Fig. 10 shows climate changes (δ^{18}O) and Hg anomalies (proxy for Deccan volcanism) during the last 70 ky of the Maastrichtian leading up to the mass extinction at Elles. No temperatures have been calculated from this δ^{18}O data because diagenetic alteration of foraminiferal shell calcite shifts values negative though temperature trends are preserved (see Supplementary materials S4). Hg in sediments is a byproduct of explosive volcanism and has a residence time of 1–2 yrs in the atmosphere during which it is distributed by winds worldwide before fallout and accumulation in sediments (Grasby et al., 2013; Thibodeau and Bergquist, 2017). Since Hg is commonly concentrated in organic carbon, it is typically normalized and shown as the ratio of Hg to total organic carbon (Hg/TOC).
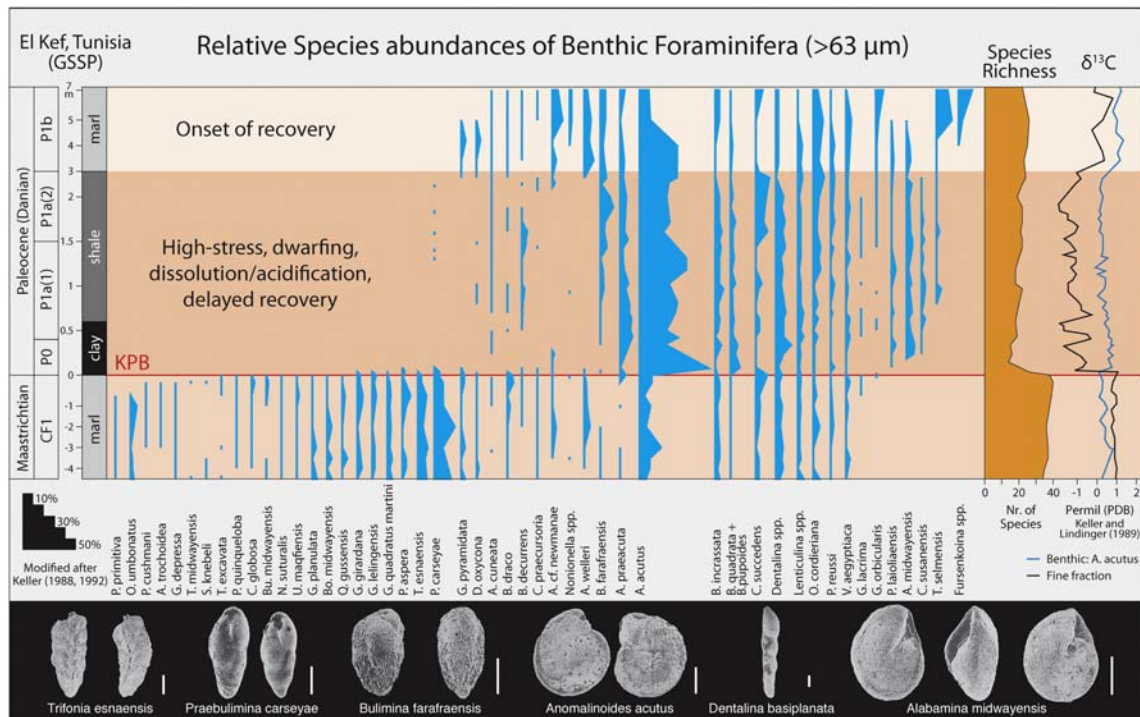

Fig. 9. Relative abundances of benthic foraminifera (>63 μm) and carbon stable isotopes of bulk rock and benthic species *Anomalinoides acutus* across the KPB transition at El Kef, Tunisia. Note the major faunal turnover across the KPB with up to 48% species disappearing over 500 ky with many of them reappearing after environmental recovery. Faunal data from Keller (1988b); stable isotope data from Keller and Lindinger (1989).
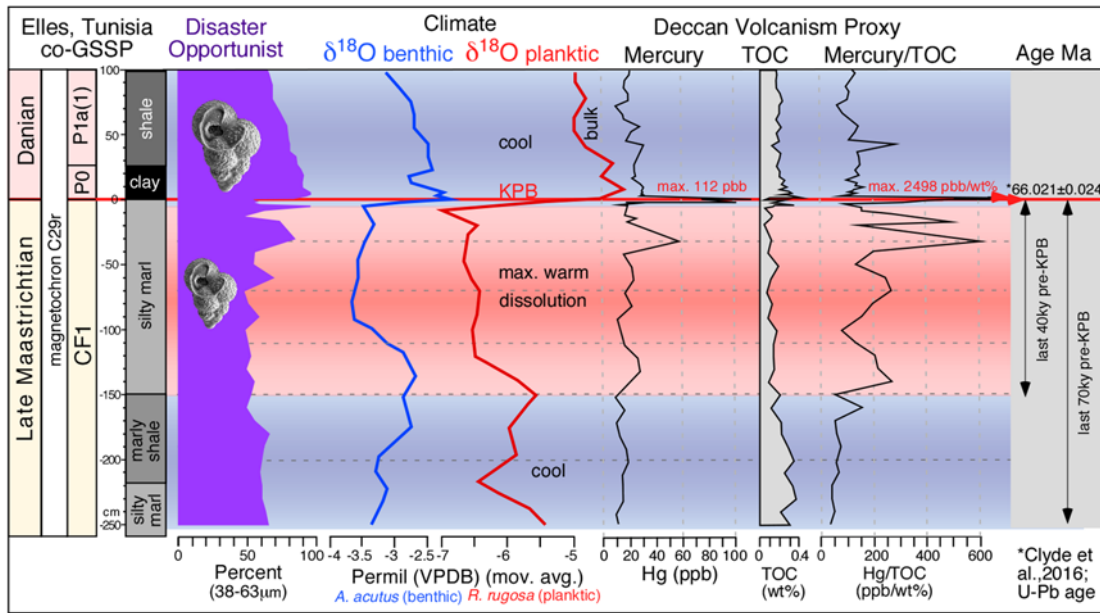
Fig. 10. Paleoenvironmental proxies (oxygen isotopes, mercury and disaster opportunist species) across the KPB at Elles, Tunisia. Note climate warming during the last 10 ky of the Maastrichtian coincides with increased Deccan volcanism (Hg/TOC ratio), which accelerates during the last thousand years and culminates with the KPB mass extinction. Hg and TOC data in Supplementary materials S2, Table S2.

The Elles δ^{18}O record indicates a relatively cool climate from 70 to 40 ky pre-KPB during a volcanically quiet period (Fig. 10). About 40 ky pre-KPB, surface water rapidly warmed coincident with major Deccan eruptions but warming in bottom waters is delayed by several thousand years. During the last 10 ky pre-KPB, climate remained warm and Hg/TOC ratios remained high. Through this interval Hg/TOC ratios mark peak volcanic activity with accelerating eruptions reaching maximum values at the KPB mass extinction (2498 ppb/wt%; 1291 ppb/wt% at El Kef).

We interpret the Hg/TOC ratios at Elles as recording Deccan eruptions with the high ratios indicating larger or more explosive eruptions.

Maximum climate warming and accelerating massive Deccan eruptions during the last 10 ky may mark the tipping point for planktic foraminifera. From this point on, extinctions are rapid culminating at the KPB. Faunal assemblages during this interval are dominated by stress-tolerant and generally dwarfed survivor taxa with the disaster opportunist *G. cretacea* being the most abundant (Figs. 5, 6A, B). At El Kef, faunal proxies indicate diversity loss, decreasing P/B ratio, increasing fragmentation in planktic foraminifera due to dissolution and high abundance of dwarfed *Guembelitria* populations (Fig. 11). Similar faunal extinctions, disaster opportunists and dissolution coincident with high Hg/TOC ratios have been recorded during the last 30–50 ky pre-KPB in France,
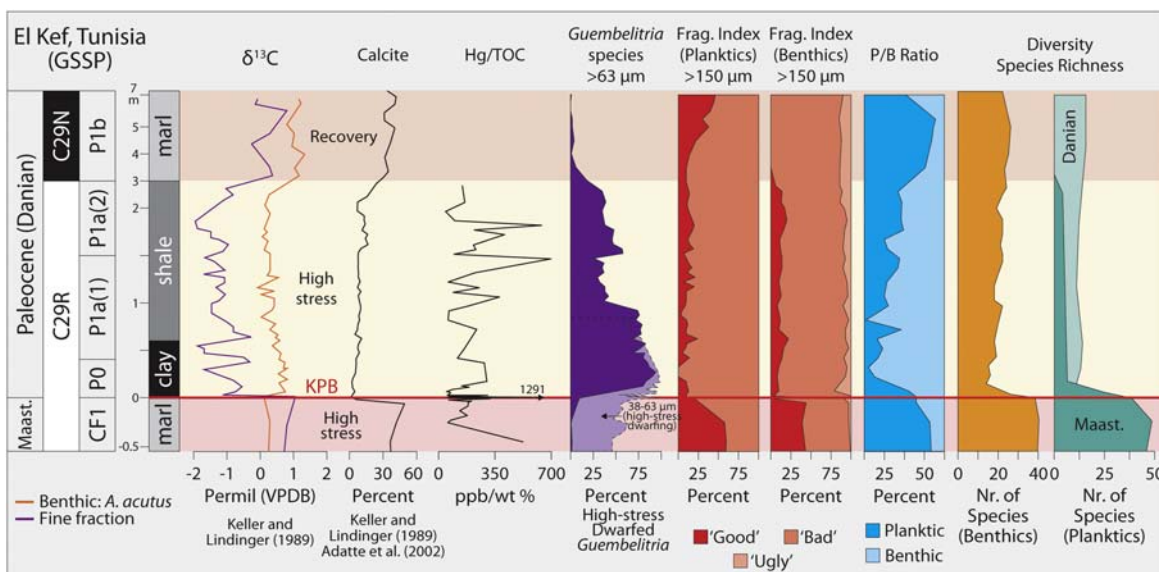

Fig. 11. Paleoenvironmental proxies for the KPB transition at El Kef, Tunisia. The interval analyzed spans part of the latest Maastrichtian warming (zone CF1) marked by ocean acidification and high dissolution effects (FI), and 500 ky of the early Danian zones P0–P1a(2) marked by continuous high-stress low oxygen conditions and ends with the onset of recovery in P1b (base C29n). Data table (Table S1) in Supplementary materials S2.

Austria and Spain and interpreted as ocean acidification (Font et al., 2016; Font et al., 2018; Punekar et al., 2016).

Ocean acidification linked to Large Igneous Province (LIP) volcanism has been identified for the PETM and mass extinctions at the KPB, end-Triassic and end-Permian (Hönisch et al., 2012). CO_2 emissions into the atmosphere from LIP volcanism can severely perturb the carbon cycle. If the rate of atmospheric pCO_2 increase overtakes the buffering time/capacity of the ocean (~1000 yrs; Zeebe, 2012), seawater carbonate chemistry can be seriously altered resulting in the lowering of carbonate ion concentration ($[CO_3^{2-}]$) and the surface ocean pH (Kump et al., 2009). Ocean acidification leads to calcification crises in shelly organisms, such as nannofossils, foraminifera, bivalves, gastropods and pteropods, and has increasingly been identified as an important mechanism linking major volcanic episodes, including the PETM and KPB, with faunal turnovers and mass extinction events (Bond and Wignall, 2014; Hönisch et al., 2012; Font et al., 2016; Punekar et al., 2016).

The most characteristic KPB signals, apart from the Ir anomaly and mass extinction, are the drop in $CaCO_3$ to near 0%, the Hg anomalies and high Hg/TOC ratios, and the 2–3‰ drop in $\delta^{13}C$, which is attributed to the mass extinction, loss of primary productivity and collapse of the biological carbon pump (Fig. 11). All faunal proxies indicate continued high-stress conditions through the early Danian C29r (~500 ky). The inverse surface-to-deep $\delta^{13}C$ gradient persisted for ~1 Myr into C29n and $CaCO_3$ remained low (<10%). During these stress conditions the disaster opportunist *Guembelitria* dominated but alternated with the evolving short-ranging opportunist *P. longiapertura* (Fig. 5). The onset of recovery resulted in the extinction of the latter, near disappearance of the former, increased abundance of earlier taxa and evolution of new species. The recovery is led by a gradual return to higher productivity ($\delta^{13}C$) and increased $CaCO_3$ (>30%) (Fig. 11). The cause for this delayed recovery has long remained an enigma. The answer appears to be continued Deccan volcanism after the mass extinction as indicated by Hg/TOC anomalies.

4. Paleocene-Eocene Thermal Maximum (PETM): DABABIYA (GSSP)

The Dababiya GSSP is located on the eastern side of the upper Nile Valley and 35 km southeast of Luxor at 25°30′N, 32°31′E (Fig. 2). Sediment deposition occurred at outer shelf depth between 150 and 200 m (Alegret et al., 2005) in a submarine channel (Fig. 12A–C). The outcrop is fragile because it forms a precarious point jutting out at the turning point between eastern and northwestern parts of the channel and a vertical fracture runs through it. The section was sampled at 50 m to the northwest and 25 m to the east of the turning point, which partially collapsed in the spring of 2016 along the vertical fracture (Fig. 12C).

Khozyem et al. (2014, 2015) published geochemical and stratigraphic studies of the two sampled sequences. Earlier publications reported on mineralogy and geochemistry (Dupuis et al., 2003; Soliman et al., 2006; Schulte et al., 2011), and planktic and benthic foraminifera (Speijer et al., 1995; Speijer and Schmitz, 1998; Speijer and Wagner, 2002; Berggren and Ouda, 2003; Alegret et al., 2005; Alegret and Ortiz, 2006). Here we present new quantitative data on the planktic foraminiferal response to the PETM event at the section 25 m east from the GSSP cliff compared with benthic foraminifera and previously published stable isotope records (Alegret and Ortiz, 2006; Dupuis et al., 2003) (Fig. 12B, C).

4.1. PEB-defining criteria

The PEB is defined based on: (1) global $\delta^{13}C_{org}$ and $\delta^{13}C_{carb}$ isotope excursions (CIE), (2) disappearance of the deep water benthic foraminifer *Stensioina beccariiformis*, (3) transient occurrence of planktic foraminifera (*Acarinina africana*, *A. sibaiyaensis*, *Morozovella allisonensis*) during the $\delta^{13}C$ excursions, (4) transient occurrence of the nannofossil *Rhomboaster* spp. – *Discoaster araneus* assemblage and (5) acme of the dinoflagellate *Apectodinium* (Aubry et al., 2007). At our Dababiya

Fig. 12. (A) Dababiya outcrop with GSSP designated cliff to the right and our sampled location 25 m to the left (East). (B) Sampling of the section using a ladder. (C) Contiguous outcrop between the GSSP cliff and our sampled section at 25 m east permits tracing the lithology bed by bed. Note the GSSP outcrop collapsed in the spring of 2016 at the vertical crack seen in C across the label "PEB". Armed guards protected the outcrop from eagerly sampling geologists.
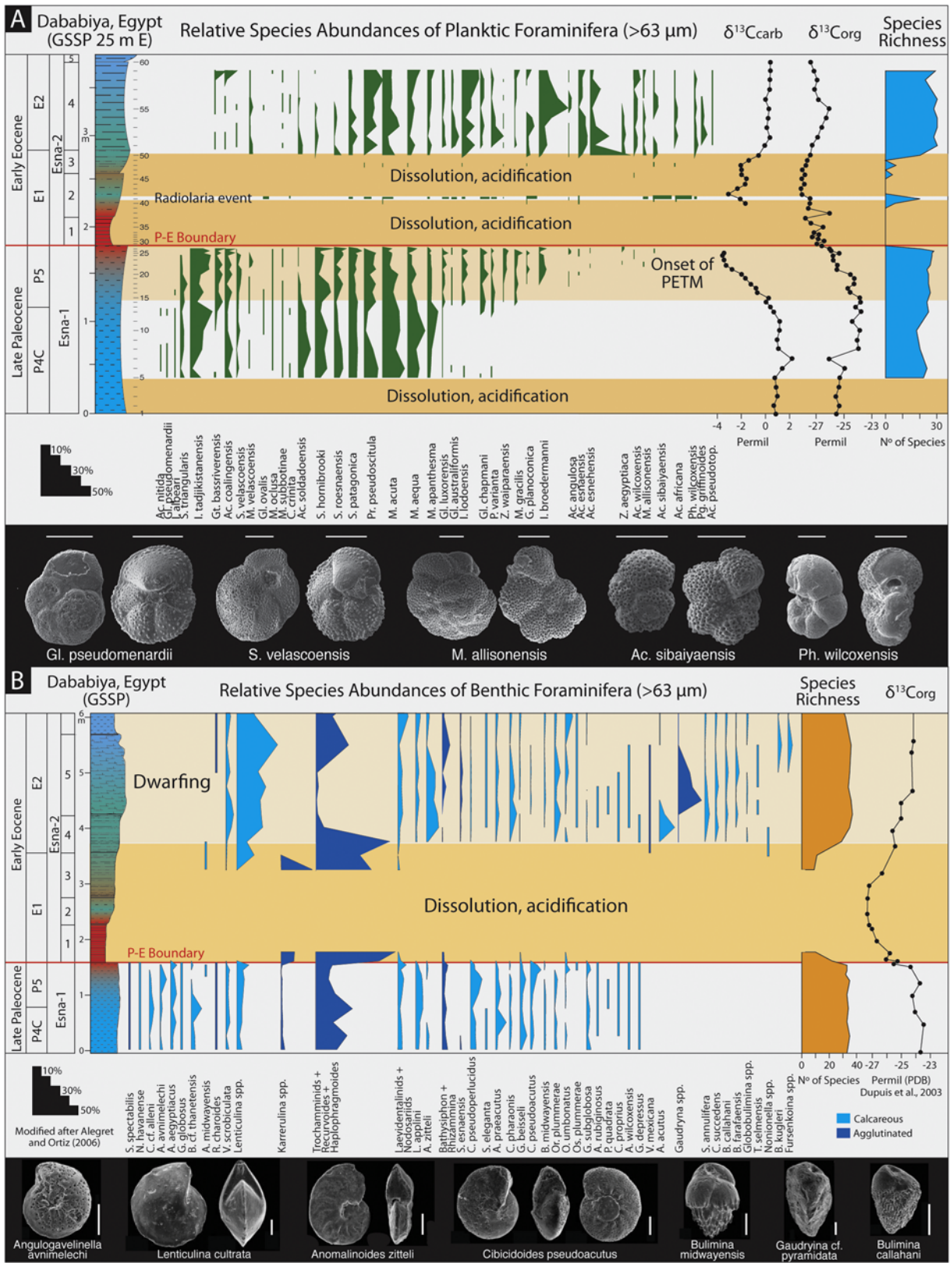
Fig. 13. (A) Relative abundances of planktic foraminifera, carbon stable isotopes and species richness at Dababiya, Egypt, 25 m east of the GSSP outcrop. The PETM interval spans from its gradual onset 75 cm below to 1 m above the PEB and is marked by near total carbonate dissolution. Another strong dissolution interval at the base of the section has common benthic species but only rare planktics. Faunal data from this study, isotope data from Khozyem et al. (2014, 2015). (B) Relative abundances of benthic foraminifera show a major faunal turnover but few species extinctions (18%, 7 species). Faunal data from Alegret and Ortiz (2006).

section 25 m east of the GSSP cliff, these PEB defining characteristics are identified. Lithology and geochemistry are discussed in Khozyem et al. (2014, 2015).

4.2. Biostratigraphy: planktic foraminifera

Biostratigraphy for the Dababiya section is based on high-resolution planktic foraminifera and the standard biozonation scheme by Olsson et al. (1999) and Pearson et al. (2006) (Fig. 13A). The sampled interval spans zones P4c, P5, E1 and E2 covering an estimated time span of 2 Myr (54.5–56.5 Ma). Zone P4c marks the base of the section as indicated by the last appearance (LA) of the index species *Globanomalina pseudomenardii* and an assemblage dominated by *Igorina tadjjikistanensis*, *Acarinina soldadoensis*, *Subbotina hornibrooki*, *Morozovella acuta* and *M. aequa*. The interval from the extinction of *Gl. pseudomenardii* to the first appearance (FA) of *Acarinina sibaiyaensis* defines zone P5 and the top of the Paleocene. At Dababiya, zone P5 marks the onset of the PETM with a 40% increase in species diversity (from 21 to 35 species) and decreased abundance of the dominant zone P5 species correlative with a gradual decrease in $\delta^{13}C_{org}$ and $\delta^{13}C_{carb}$ values culminating at the PEB (Fig. 13A).

Above the PEB, zone E1 spans 1 m with the basal 42 cm a barren clay devoid of CaCO$_3$ marking dissolution/ocean acidification (Fig. 13A). Between 42 and 47 cm is a 5 cm thick radiolarian-rich interval with the transient PETM fauna dominated by *A. sibaiyaensis* and *A. africana* and FA of *A. africana* and *Morozovella allisonensis*. The 50 cm above mark the onset of recovery with increasing $\delta^{13}C$ values and rare foraminifera in the upper 20 cm. The E1/E2 boundary is placed at the first continuous occurrence of *Pseudohastingerina wilcoxensis* 1 m above the PEB coincident with the reappearance of diverse assemblages that existed already during the latest Paleocene. Just four species disappeared as they morphed into new species - a phenomenon known as pseudoextinction. Returning species have generally larger shell sizes than before their temporary disappearance, show morphological diversification and speciation (Lu and Keller, 1993, 1995a, 1995b; Lu et al., 1998; Kaiho et al., 2006; Kelly et al., 1996, 1998; Pardo et al., 1999; Berggren and Ouda, 2003; Luciani et al., 2007, 2016; Khozyem et al., 2014). Thus, despite major climate warming, decreased productivity and ocean acidification, the PETM caused no significant species extinctions, likely due to migration into higher latitudes during warming, and fostered major diversification in its aftermath.

4.3. Benthic extinction and faunal turnover event

Alegret et al. (2005, Alegret and Ortiz, 2006) reported a major benthic faunal turnover at the Dababiya section (Fig. 13B) but only 7 species (18%) went extinct, 82% were survivors that reappeared after the PETM acidification event, and 26% new species evolved during environmental recovery. Similar observations are reported from marginal and epicontinental seas (Speijer and Schmitz, 1998; Speijer and Wagner, 2002). But in lower bathyal to abyssal environments (e.g., Alamedilla, Spain) species extinctions reached ~37% (Alegret et al., 2009), which is in the lower estimate of the previously reported extinction ranging between 30 and 50% (Thomas, 1998). Thus, significant benthic extinctions were restricted to deep-water environments and generally concentrated at the onset of the PETM event. This can be explained by the observed shoaling of the CCD by 2000 m during the PETM (Zachos et al., 2008).

5. Environmental proxies: PEB

The PETM is marked by a global temperature increase of 5–9 °C over an interval variously estimated ~10 ky or ~30 ky and estimated loading of 2000 Gt of isotopically light carbon to the atmosphere and oceans (Zachos et al., 2003, 2005, 2006; Sluijs et al., 2006; Weijers et al., 2007). A low correlation coefficient of CaCO$_3$ vs. $\delta^{13}C_{carb}$ ($R^2 = 0.025$) indicates limited diagenetic overprinting on the $\delta^{13}C_{carb}$ values but

$\delta^{18}O$ data are strongly affected by diagenesis (see Supplementary materials S4, Fig. S11).

Faunal, geochemical and volcanic proxies illustrate the high-stress conditions across the PETM (Fig. 14). At the base of the section (zone P4C), a short dissolution event is marked by near-absence of planktic species, decreased CaCO$_3$ from 50% to 40% and maximum Hg/TOC ratios. In contrast, benthic species are well preserved. This suggests surface ocean acidification as a result of peak volcanic emissions (NAIP). Above this interval planktic and benthic species show dissolution effects with just 1/3 well-preserved 'good' planktic and between 20 and 60% 'good' benthic foraminifera. Hg/TOC ratios as well as $\delta^{13}C_{carb}$ and $\delta^{13}C_{org}$ values gradually decreased reaching minimum values 20 cm below the PEB and at the PEB, respectively (Fig. 14).

A similar gradual $\delta^{13}C_{org}$ decrease has been reported from Alamedilla, Spain, (Lu et al., 1996) and Spitsbergen, Norway, with the latter linked to North Atlantic Igneous Province (NAIP) volcanism (Wieczorek et al., 2013). At Dababiya Hg/TOC ratios (ppb/wt%) also link this interval to NAIP. At all three sites the isotopic records are interpreted as gradually increasing ocean temperatures due to atmospheric CO$_2$ loading linked to NAIP (Speijer and Wagner, 2002; Sluijs et al., 2008; Bowen and Zachos, 2010; Khozyem et al., 2015).

At the PEB planktic foraminifera suddenly disappeared and calcite decreased to near 0% for 42 cm in the lower part of zone E1 followed by a brief reappearance of calcite (35%) and small opportunistic new foraminiferal species and radiolarians (Figs. 13A, 14). Above this interval calcite varies between 10 and 30% but planktic foraminifera are generally rare to absent and reappearing only with calcite content >40% at the top of zone E1 (Fig. 14).

The sudden calcite drop at the PEB from 50% to near 0% coincides with onset of high detrital input during the PETM interval that spans zone E1 (Figs. 13, 14). Khozyem et al. (2015, p. 127) argued that "*detrital input negatively affects the calcite content resulting in minimum values that could be due to leaching of carbonate contents under acid conditions and/or dilution by increased detrital input.*" The high terrigenous input at Dababiya due to climate and sea level changes supports this interpretation (e.g., Khozyem et al., 2015; Schulte et al., 2011; Speijer and Wagner, 2002). The temporary absence of benthic and planktic foraminifera and near absence of nannofossils during the PETM coupled with shoaling of the CCD by 2000 m indicates ocean acidification likely due to a huge rapid input of CO$_2$ from methane degassing (e.g., Zachos et al., 2008; Westerhold et al., 2011) and/or from NAIP volcanism (Gutjahr et al., 2017).

6. Discussion

6.1. PETM event

During the Paleocene-Eocene transition two major volcanic events temporally precede and overlap the PETM (~55.8 ± 0.2 Ma; Westerhold et al., 2009; Charles et al., 2011; Wieczorek et al., 2013) (Fig. 1B): (1) the North Atlantic Igneous Province (NAIP) formed during the opening of the northern part of the North Atlantic ocean ~61 Ma with maximum activity between 57 and 54 Ma (Hirschmann et al., 1997; Svensen et al., 2004, 2010; Storey et al., 2007); and (2) Central American circum-Caribbean volcanism linked to enhanced tectonic activity that began ~56–55.5 Ma in the proto Greater Antilles (Sigurdsson et al., 1997). Thus the nature of NAIP volcanism associated with the PETM event was fundamentally different from the continental flood basalt Deccan Traps eruptions.

Support for NAIP as driver for the PETM comes from a large drop in $^{187}Os/^{188}Os$ and ash deposits dated ~24 ky before the maximum $\delta^{13}C$ excursion in Core BH9/05 (Spitsbergen, Svalbard Archipelago, Norway) (Wieczorek et al., 2013) and from an Earth system model pairing ocean surface pH data and a carbon isotope record from the northeast Atlantic Ocean (Gutjahr et al., 2017). Recent discovery of Hg anomalies in North Atlantic, Spain and Egypt (Khozyem et al., 2017) provide further
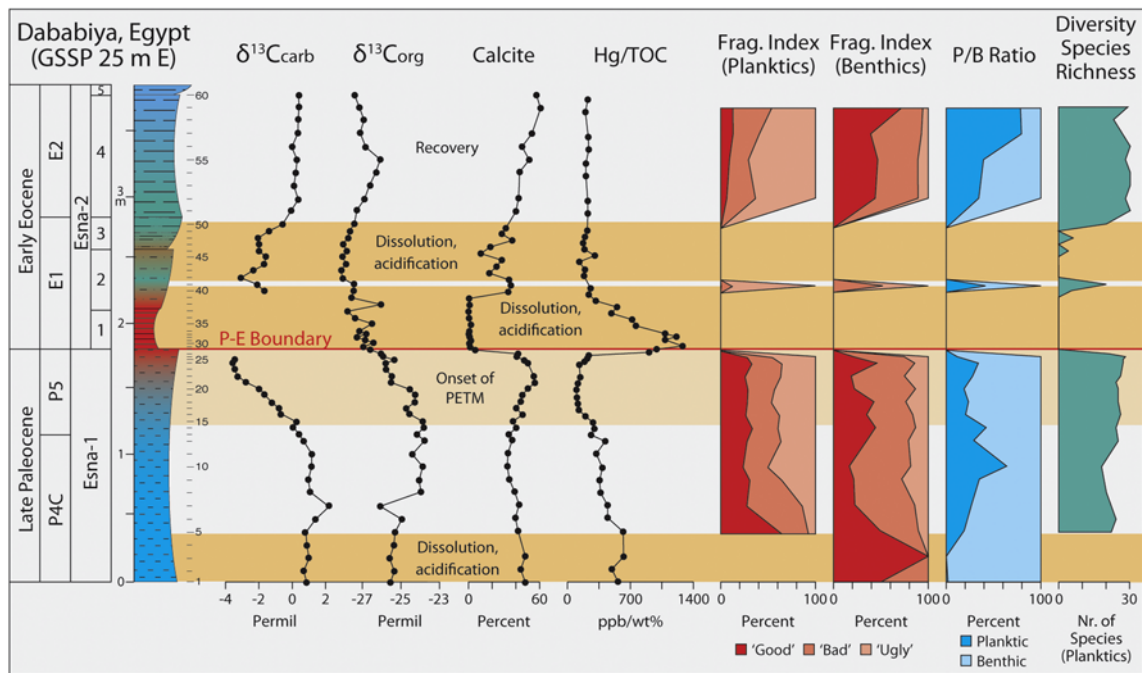
Fig. 14. Paleoenvironmental proxies for the PETM transition at Dababiya, Egypt. Dissolution first appears in zone P4C coincident with high Hg/TOC values. The onset of the PETM begins with gradually decreasing $\delta^{13}C$ values in zone P5 that reached maximum at the PEB. Near total $CaCO_3$ dissolution in the lower part of zone E1 and strong dissolution in the upper part marks an interval nearly devoid of marine calcareous plankton during the PETM and signals strong ocean acidification despite the onset of recovery in $\delta^{13}C$ and $CaCO_3$. Faunal recovery begins in zone E2 with increasing $\delta^{13}C$ values and $CaCO_3$ reaching 60%. Data table (Table S3) in Supplementary materials S2.

evidence linking NAIP to the PETM event by initiating the warming that likely led to the release of methane gases from organic-rich sediments (Svensen et al., 2004, 2010; Maclennan and Jones, 2006; Wieczorek et al., 2013).

The PETM event was a short-term and isolated event possibly triggered by an estimated ~2000 Gt of CO_2 from volcanic activity (NAIP, Sinton and Duncan, 1998; Westerhold et al., 2011) and ~1500 Gt of methane carbon from gas hydrates released into the atmosphere (Dickens et al., 1995; Dickens, 2003). (These CO_2 estimates are based on the $\delta^{13}C$ isotope excursion, which may have large uncertainties.) The resulting rapid global warming is thought to have occurred over about ~10 ky with the entire event lasting ~170 ky. This suggests rapid injection of carbon and slow subsequent removal given that the average residence time of carbon in the ocean is about 100 ky (Zachos et al., 2005, 2008). Boron-based ($\delta^{11}B$ and B/Ca) proxies for surface ocean carbonate chemistry indicate an estimated ~0.3 units drop in the pH of surface and thermocline seawater sustained over ~70 ky during the PETM (Penman et al., 2014). Model simulations suggest that this duration is consistent with a scenario of rapid initial pulse of carbon loading followed by continued slow, gradual release of carbon likely due to feedbacks (Panchuk et al., 2008; Zeebe et al., 2009; Zeebe, 2012).

The PETM coincides with ocean acidification and shoaling of the CCD by 2000 m (Zachos et al., 2005, 2008; Speijer and Wagner, 2002; Sluijs et al., 2008; Gutjahr et al., 2017); the latter may account for benthic foraminifera extinctions in deep waters (Thomas, 1998; Alegret and Ortiz, 2006). Planktic foraminifera and calcareous nannofossils temporarily disappeared from tropical and subtropical oceans (suggesting warming and surface ocean acidification) by migrating into higher latitudes. Assemblages returned after the PETM with no significant extinctions and underwent evolutionary diversification (Lu and Keller, 1993, 1995a, 1995b; Kelly et al., 1996, 1998; Luciani et al., 2007, 2016; Khozyem et al., 2014). On land extreme climate warming resulted in decreased abundances and dwarfing ranging from soil dwelling species (e.g., burrowers, crayfish, mollusks, Smith et al., 2009) to mammals (D'Ambrosia et al., 2017). But the great mammal migration, diversification and geographic dispersal began shortly after the PETM (Koch et al., 1992,

1995; Hooker, 1998; Clyde and Gingerich, 1998; Clyde et al., 2003; Tong and Wang, 2006; Smith et al., 2006; Rose et al., 2008; Punekar and Saraswati, 2010; Smith, 2012).

6.2. KPB event

The main phase of Deccan volcanism spans magnetochron C29r (Chenet et al., 2008, 2009) dated ~750 ky during which time an estimated >1.1 million km^3 of basalt erupted (Schoene et al., 2015). The KPB is at 66.021 ± 0.024 Ma, ~350 ky after the onset of eruptions at the base of C29r. Hg anomalies and Hg/TOC ratios at Elles indicate that volcanic eruptions accelerated during the last 60 ky before the mass extinction (Fig. 10). In the field in India, Deccan eruptions near the end of the Maastrichtian resulted in 3–4 lava megaflows that flowed over 1000 km across India into the Bay of Bengal (Keller et al., 2011a; Self et al., 2008) (Fig. 1A). The mass extinction of planktic foraminifera was documented directly in sediments between these lava megaflows in cores 2500–3500 m below the surface in the Krishna-Godavari Basin (Keller et al., 2011a, 2012). Danian (zone P1a) sediments overlie the megaflows and constrain the age of the KPB mass extinction to peak volcanic activity, as now confirmed by the large Hg/TOC ratios at Elles (Fig. 10). An estimated cumulative loading of 12,000–28,000 Gt of volcanogenic CO_2 spewed into the end-Cretaceous atmosphere within <350 ky and significantly increased atmospheric pCO_2 (Courtillot and Fluteau, 2014; Self et al., 2014). Volcanic eruptions continued intermittently through the early Danian C29r with the last phase of eruptions in the lower part of C29n (Fig. 11). Mercury analysis in marine and terrestrial sediments worldwide mark late Maastrichtian and early Danian Deccan eruptions linked directly to the KPB mass extinction (Font et al., 2016, 2018).

Rapid climate warming of 3–4 °C during massive Deccan eruptions resulted in dwarfed planktic foraminifera and reduced abundances of all but a few stress-resistant taxa dominated by a single disaster opportunist and sole long-term survivor *Guembelitria cretacea* (Keller and Abramovich, 2009). On land, non-avian dinosaurs, mammals, amphibians, plants and insects (e.g., MacLeod et al., 1997; Labandeira et al., 2002; Wilf and Johnson, 2004; Wilson, 2005, Wilson et al., 2014;

Table 1

Comparison of KPB, PETM and Anthropocene events based on climate and environmental changes shows great similarities, except that the Anthropocene warming is orders of magnitude more rapid than the PETM and KPB warming. The rate of faunal turnover and particularly extinctions is very difficult to estimate and contains the largest potential errors. At the current rate of CO_2 input into the atmosphere, the Anthropocene extinction is estimated to reach the 75% mass extinction level possibly within the next 100 years or optimistically within the next 250–500 yrs.

Events	Anthropocene: mass extinction?	Paleocene/Eocene: PETM	End-Cretaceous: mass extinction
Age (Ma)	Ongoing, predicted within 250-500 yrs[a]	55.8 ± 0.2 Ma	66.021 ± 0.024 Ma
Faunal turnover	Ongoing extinctions	Extinctions/originations	Mass extinction
Mass extinctions	In progress	Minor[b]	~50% genera, ~75% species
Rate of extinctions	In accelerating phase 20–50× background rates[a]	Rapid at max. warming 6–12× background rates in benthic foraminifera[b]	Rapid over ~1000 years ~220× background rate in planktic foraminifera[c]
Benthic foram extinctions	Yes, ongoing	30–50% species	Minor
Planktic foram extinctions	Yes, ongoing	Minor	99% species
Vertebrate extinctions	Yes, ongoing	Minor, migration	Major
Terrestrial extinctions	Yes, ongoing	Minor	Major
Recovery	–	Rapid after PETM	Delayed >500 ky
Pre-event climate	Gradual warming	Gradual warming	Rapid warm-cool changes over 350 ky[d]
Climate (greenhouse gases)	Rapid warming	Rapid warming	Rapid warming
Warming: rate	1–4 °C/100 yrs, 2–10 °C next 200–300 yrs	0.025 °C/100 yrs, total 5 °C[e]	Oceans 3–4 °C[d] Land 6–8 °C[f]
Warming: max duration	Decades to 100's of years	Tens of thousands of years	Tens of thousands of years
Tipping point temperature increase >4 °C	~4 °C possibly reached by 2020	5 °C	~5 °C
Sea-level	Rapid rise (1–2 m)[g]	Rapid rise (3–5 m)	Rise ~50 m over 100 ky
Anoxia/dysoxia	Yes	Yes, continental shelf	Dysoxia in water column
Ocean acidification (rate)	Yes (0.3 units/100 yrs)[h]	Yes (0.3 units/20 ky)[i]	Yes[j]
Clathrates (CH_4)	No (possible in future)	Yes	None confirmed
Volcanism (LIPs)	No	North Atlantic Igneous Province (NAIP)	Deccan Traps
Global warming: main underlying cause(s)	CO_2: fossil fuel burning CH_4: peat, coal, permafrost	CO_2: volcanoes CH_4: clathrates, peat, coal, permafrost	CO_2: volcanoes CH_4: no data
Impacts	No	Unconfirmed	Chicxulub 180 km

[a] Anthropocene extinctions are predicted to reach the 75% mass extinction level within the next 250 to 500 yrs (conservative estimate) based on projection of current rates of extinctions and current rates of fossil fuel burning (e.g. May et al., 1995; Hughes et al., 1997; Ceballos and Ehrlich, 2002; Pereira et al., 2010; Barnosky et al., 2011).

[b] For the PETM event extinctions are limited to benthic foraminifera in the marine realm; with maximum 50% extinct over 170 ky (estimated duration of PETM event), the rate of extinction estimated from El Kef is 0.12 species/ky or about 12–24 background rates at 1–2 species/100 ky (this study).

[c] Estimated from planktic foraminifera: 66% (44 species) extinct over about 10 ky, an average of 4.4 species/ky; background rates are 1–2 species/100 ky or 0.01–0.02/ky. This means that the rate of extinction is at least 220 times background. About 33% go extinct within 50–100 ky after the KPB leaving a single survivor species (this study).

[d] e.g., Stüben et al. (2003), Li and Keller (1998), Abramovich and Keller (2003), Punekar et al. (2014).

[e] Zachos et al. (2005, 2006).

[f] Wilf et al. (2003), Nordt et al. (2003).

[g] IPCC 5th Assessment Report (2013), conservative estimate.

[h] e.g., Sluijs et al. (2008), IPCC 4th Assessment Report (2007), projected global average pH surface ocean, between 2000 and 2100.

[i] Penman et al. (2014), comparison of $\delta^{11}B$ data and LOSCAR model simulation.

[j] Font et al. (2011, 2014), Punekar et al. (2016).

Nichols and Johnson, 2008; Longrich et al., 2011, 2012; Wilson, 2014; Vajda and Bercovici, 2014; Donovan et al., 2016) also recorded a prolonged ecological decline, reduced diversity and turnovers during

climate instability associated with Deccan volcanism preceding the KPB (e.g., Wilf and Johnson, 2004; Wilson, 2005, 2014; Wilson et al., 2014; Archibald, 1996, 2011).

The similar patterns of long-term stress and decline in marine and terrestrial faunas and flora during the late Maastrichtian C29r warming parallels massive Deccan volcanism that accelerated during the last 10 ky leading to further warming and probably reaching threshold conditions. Maximum volcanic eruptions in rapid succession during the last few thousand years culminated with the KPB mass extinction (Fig. 10). The subsequent delayed recovery in marine plankton and on land can now be shown to coincide with continued though less frequent Deccan volcanic eruptions keeping stress conditions high (Fig. 11). Deccan volcanism is thus a major culprit for climate warming, biotic stresses and the mass extinction.

The Chicxulub impact is commonly believed to be the sole cause for the KPB mass extinction based primarily on the Ir anomaly in the KPB clay layer, the impact crater in Mexico and impact glass spherules frequently found in sediments at, below or above the KPB, which has been the source of controversy (Schulte et al., 2010; Keller et al., 2011b). (See Supplementary materials S3 for a discussion of this controversy.) However, over the past 10 years, increasing evidence linking the mass extinction to Deccan volcanism reveals the need for re-evaluation of the impact theory. Critical evidence linking the mass extinction directly to Deccan volcanism includes: (1) the mass extinction documented between massive lava flows in India directly below the KPB (Keller et al., 2008, 2009, 2011a, 2012), (2) U-Pb age dating of ash layers and red bole intertrappean sediments that span C29r (Schoene et al., 2015), and (3) Hg anomalies that mark atmospheric fallout from Deccan eruptions worldwide (Silva et al., 2013; Font et al., 2016; this study). As a result, the impact theory is already being modified by impact proponents suggesting that the impact triggered Deccan volcanism (Richards et al., 2015), or accelerated Deccan volcanism leading to extinctions (Renne et al., 2015). The precise age of the Chicxulub impact is currently under investigation based on new Ar/Ar dating of impact spherules by three laboratories, although accuracy is limited to within 200 ky and therefore cannot resolve the presumed KPB age. The precise role the impact played in the mass extinction also still remains to be determined in light of new Deccan volcanism data. What is certain is that this impact added a significant blow to an already weakened and stressed environment regardless of the precise age. But it was a one-time blow at the level of total CO_2 and SO_2 gas output comparable to one major Deccan eruption pulse of which there are many (Chenet et al., 2008; Courtillot and Fluteau, 2014).

At present we can confidently evaluate the PETM and KPB catastrophes based on the response by planktic foraminifera, which are an essential part of the food chain, and new Hg anomaly data now link these global faunal records to NAIP and Deccan volcanism. The fundamentally different biotic responses to these catastrophes lie in the nature of volcanic eruptions. During the PETM, NAIP volcanism due to rifting of the North Atlantic led to relatively short-term gradual warming that likely triggered the postulated methane release and rapid warming. Absence of Hg anomalies after the PETM indicates no significant NAIP eruptions, climate cooled and biotic recovery was
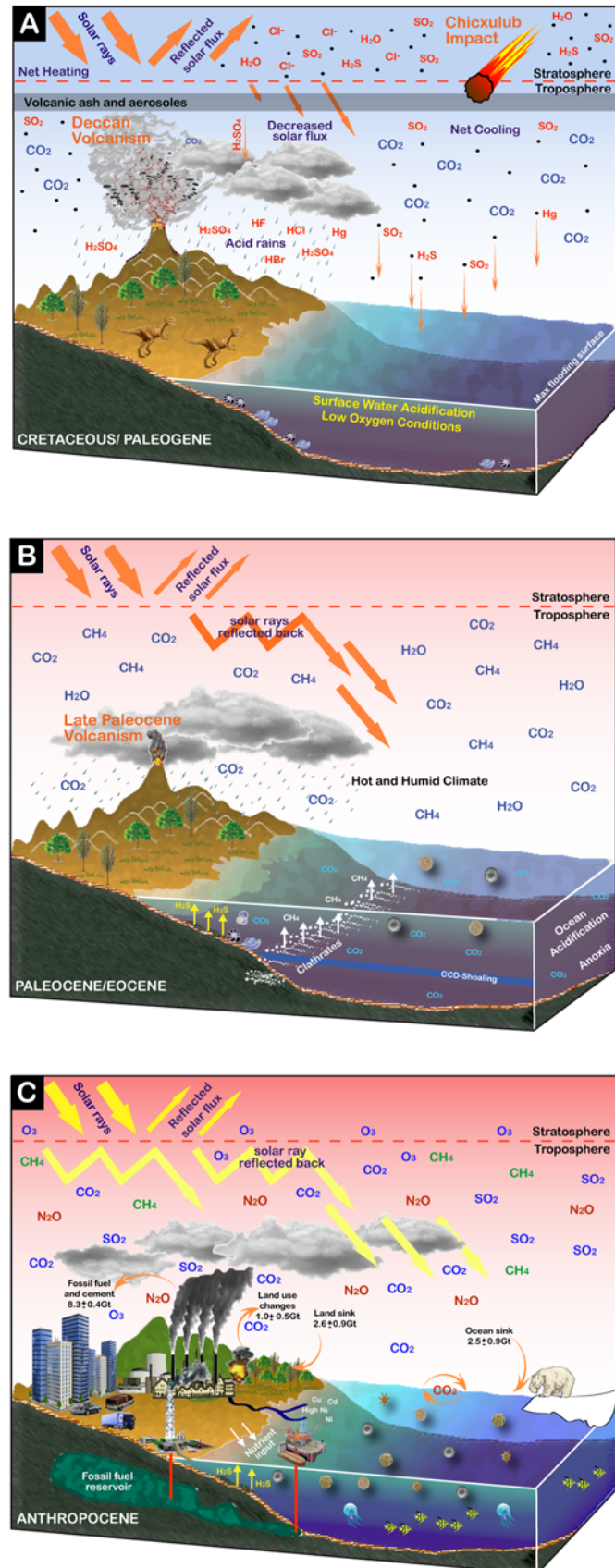
Fig. 15. Illustration of the KPB mass extinction, the PETM and Anthropocene climate warming. (A) During the latest Maastrichtian environmental devastation is mainly due to volcanism (ash, aerosols and greenhouse gases), resulting in rapid climate changes, acid rains and ocean acidification that is exacerbated by the Chicxulub impact, thus impeding calcification by marine plankton at the base of the food chain. (B) During the latest Paleocene to early Eocene: Gradual climate warming preceding the PEB is attributed to North Atlantic Igneous Province volcanism (NAIP), but the rapid warming of 5 °C (PETM) is linked to methane hydrates released from continental shelves resulting in acid rain on land and ocean acidification (~170 ky). (C) During the Anthropocene large inputs of greenhouse gases (CO_2, SO_2, N_2O) linked to human activities and fossil fuel burning leads to rapid warming and ocean acidification at a rate exceeding those at the PETM and KPB by orders of magnitude. Global carbon budget data for the Anthropocene from Le Quéré et al. (2013). Illustration modified from Glikson (2014).

rapid. In contrast, Deccan Traps are continental flood basalt eruptions that began ~350 ky before the KPB mass extinction causing long-term warming. Accelerating eruptions during the last ~10 ky reached the tipping point and mass extinction. Thereafter, intermittent Deccan eruptions delayed recovery for over 500 ky.

6.3. Anthropocene: the sixth mass extinction?

Scientists increasingly recognize the accelerating rate of modern species extinctions and sounding alarm that humans are now causing the sixth mass extinction (e.g., Leakey and Lewin, 1992; Dirzo and Raven, 2003; Wake and Vredenburg, 2008; Barnosky et al., 2011; Glikson, 2014). Evidence of an impending catastrophe is all around us in the increasing rate of species extinctions and those endangered on the verge of extinction. Climate warming due to fossil fuel burning is attributed to the increasing rate of extreme climate events, melting of polar glaciers and rapidly rising sea level. Despite all this, it is hard to fathom that we are living in the midst of a mass extinction.

We can glimpse our future from comparison with extreme events in the past, particularly the hyperthermal warming (PETM) of the Paleocene-Eocene boundary (PEB, 55.8 Ma) and rapid extreme warming leading to the end-Cretaceous mass extinction (KPB, 66.02 Ma) (Table 1). Both PEB and KPB catastrophes are largely the results of massive rapid emissions of greenhouse gases leading to the tipping point. At one extreme, scientists suggest the tipping point may have already been reached at the current CO_2 level (407 ppm) and that just 1 °C additional warming may result in runaway warming, ocean acidification and the sixth mass extinction (Glikson, 2014). At the other extreme are those who deny the existence of current climate change.

Projecting current and/or increasing Anthropocene warming into the future has the potential to follow the path of the PETM hyperwarming and faunal turnover, as frequently suggested by scientists, or it could end in a mass extinction similar to the KPB as suggested by predictions of the sixth mass extinction. Global climate warming due to massive input of greenhouse gases is the leading cause for all three events even if the sources differ (Table 1). Critical is the rapid rate of climate warming that is vastly (12 to 16 times) more rapid for the Anthropocene. The tipping point may be around 5 °C and just 1 °C off from the current overall temperature rise (Hay, 2011).

Ocean acidification and acid rain on land had catastrophic effects for PETM and KPB events and similar effects are already ongoing today. For example, seasonal aragonite undersaturation observed in surface waters of the Southern Ocean already have harmful effects on live pteropods (Bednarsek et al., 2012; Hunt et al., 2008; Sunday et al., 2014). By 2030 undersaturation is predicted to spread to ~30% of the Southern Ocean and >70% by 2100 as a result of anthropogenic CO_2, thus severely affecting the marine food chain (McNeil and Matear, 2008; Hauri et al., 2016).

A cartoon illustrates the nature of the three events (Fig. 15). Climate warming and the end-Cretaceous mass extinction are closely linked to the Chicxulub impact and Deccan volcanism (Fig. 15A). The latter emitted huge quantities of aerosols and greenhouse gases (CO_2, SO_2) into the atmosphere over 350 ky and the impact added in a single instant a quantity about equal to one major Deccan eruption pulse although a KPB age of this impact remains controversial (Chenet et al., 2008; Courtillot and Fluteau, 2014). Accelerating large volcanic eruptions during the last 10 ky prior to the mass extinction led to increased warming and the tipping point resulting in the rapid mass extinction of 66% planktic foraminiferal species during the last few thousand years of the Cretaceous, followed by another 33% within 50–150 ky in the early Danian. Continued eruptions in the early Danian delayed full recovery for over 500 ky.

The PEB event can be attributed to NAIP volcanism and climate warming that likely set the conditions for the abrupt release of methane (CH_4) stored in organic-rich sediments on land and continental shelves resulting in the rapid PETM warming of 5 °C within ~10 ky (Fig. 15B). Methane, partially oxidized in the water column leading to ocean acidification during the relatively short but intense PETM event (~170 ky)

raising the CCD by 2000 m. Prevailing hot-humid conditions on land and recovery of carbonate deposition via CO_2 drawdown by organic matter burial in the oceans are likely causes for the rapid return/recovery and diversification of marine faunas after the PETM (Bains et al., 2000).

Current rapid warming is the result of huge inputs of greenhouse gases (CO_2, CH_4) linked to human activities and fossil fuel burning during the Anthropocene (Fig. 15C). The input rate of greenhouse gases exceeds those at the PETM and KPB by orders of magnitude. Ozone depletion and particle pollution from fossil fuel burning and other human activities result in dust clouds that trap solar radiation in Earth's atmosphere with little reflected back into space, thus contributing to Earth's rising temperature. Similar to PEB and KPB events, today's CO_2 from the atmosphere is absorbed in the oceans and has already lowered the pH; ocean acidification is already affecting shelly organisms at the base of the food chain (e.g., pteropods, corals) and endangering all life up the food chain. At the current trend of greenhouse gas emissions, the prediction is that Cretaceous-like climate could be reached by 2070 setting us well on the way to the sixth mass extinction within as little as a couple of hundred years (Hay, 2011; Hauri et al., 2016).

The worst-case scenario could thus be similar to the KPB mass extinction but with a faster rate of extinctions; this is currently predicted as the Anthropocene mass extinction – or sixth mass extinction. The best-case scenario could be similar to the PETM event: We escape mass extinctions but suffer through a period of extreme environmental stress marked by intense heat, extreme climate events, rising sea level and severe food shortages reducing populations and forcing migration to higher latitudes for survival. This scenario depends on dramatically reducing greenhouse gas input thus slowing the rate of global warming and its dire long-term consequences.

7. Conclusions

The PETM extreme warming is a commonly used analogue and predicted best-case scenario for the current rapid climate warming in the coming decades and centuries. If this is our fate, survival is possible although in reduced populations with the best chances for survival in higher latitudes. The predicted worst-case scenario for the current climate trend is the sixth mass extinction. The KPB mass extinction is a good analogue for this catastrophic scenario because accelerating Deccan volcanic eruptions and increasing greenhouse gas input into the atmosphere can have similar effects on the biosphere as current fossil-fuel burning. Perhaps all it takes to realize the sixth mass extinction scenario is continued or increasing greenhouse gas input reaching the tipping point. It is unclear whether current climate warming will follow the PETM or KPB analogue, or a completely different model of biosphere destruction unseen in Phanerozoic mass extinctions.

Supplementary data to this article can be found online at https://doi.org/10.1016/j.gr.2017.12.002.

References

Abramovich, S., Keller, G., 2002. High stress late Maastrichtian paleoenvironment: inference from planktonic foraminifera in Tunisia. Palaeogeography, Palaeoclimatology, Palaeoecology 178:145–164. https://doi.org/10.1016/S0031-0182(01)00394-7.

Abramovich, S., Keller, G., 2003. Planktonic foraminiferal response to the latest Maastrichtian abrupt warm event: a case study from South Atlantic DSDP Site 525A. Marine Micropaleontology 48:225–249. https://doi.org/10.1016/S0377-8398(03)00021-5.

Abramovich, S., Keller, G., Stüben, D., Berner, Z., 2003. Characterization of late Campanian and Maastrichtian planktonic foraminiferal depth habitats and vital activities based on stable isotopes. Palaeogeography, Palaeoclimatology, Palaeoecology 202:1–29. https://doi.org/10.1016/S0031-0182(03)00572-8.

Abramovich, S., Yovel-Corem, S., Almogi-Labin, A., Benjamini, C., 2010. Global climate change and planktic foraminiferal response in the Maastrichtian. Paleoceanography 25, PA2201. https://doi.org/10.1029/2009PA001843.

Alegret, L., Ortiz, S., 2006. Global extinction event in benthic foraminifera across the Paleocene/Eocene boundary at the Dababiya Stratotype section. Micropaleontology 52 (5): 48–63. https://doi.org/10.2113/gsmicropal.52.5.433.

Alegret, L., Ortiz, S., Arenillas, I., Molina, E., 2005. Paleoenvironmental turnover across the Paleocene/Eocene Boundary at the Stratotype section in Dababiya (Egypt) based on benthic foraminifera. Terra Nova 17, 526–536.

Alegret, L., Ortiz, S., Molina, E., 2009. Extinction and recovery of benthic foraminifera across the Paleocene–Eocene ThermalMaximum at the Alamedilla section (Southern Spain). Palaeogeography, Palaeoclimatology, Palaeoecology 279:186–200. https://doi.org/10.1016/j.palaeo.2009.05.009.

Archibald, J.D., 1996. Testing extinction theories at the Cretaceous-Tertiary boundary using the vertebrate fossil record. In: MacLeod, N., Keller, G. (Eds.), Cretaceous-Tertiary Mass Extinctions: Biotic and Environmental Changes. WW Norton & Company, New York/London, pp. 373–397.

Archibald, J.D., 2011. Extinction and Radiation: How the Fall of Dinosaurs Led to the Rise of Mammals. JHU Press, p. 108.

Ashckenazi-Polivoda, S., Abramovich, S., Almogi-Labin, A., Schneider-Mor, A., Feinstein, S., Püttmann, W., Berner, Z., 2011. Paleoenvironments of the latest Cretaceous oil shale sequence, Southern Tethys, Israel, as an integral part of the prevailing upwelling system. Palaeogeography, Palaeoclimatology, Palaeoecology 305 (1):93–108. https://doi.org/10.1016/j.palaeo.2011.02.018.

Aubry, M.-P., Ouda, K., Dupuis, C., Berggren, W.A., Van Couvering, J.A., the Members of the Working Group on the Paleocene/Eocene Boundary, 2007. Global Standard Stratotype – Section and Point (GSSP) for the base of the Eocene Series in the Dababiya Section (Egypt). Episodes 30 (4), 271–286.

Bains, S., Norris, R.D., Corfield, R.M., Faul, K.L., 2000. Termination of global warmth at the Palaeocene/Eocene boundary through productivity feedback. Nature 407:171–174. https://doi.org/10.1038/35025035.

Barnosky, A.D., Matzke, N., Tomiya, S., Wogan, G.O., Swartz, B., Quental, T.B., Marshall, C., McGuire, J.L., Lindsey, E.L., Maguire, K.C., Mersey, B., 2011. Has the Earth's sixth mass extinction already arrived? Nature 471 (7336), 51–57.

Barrera, E., Keller, G., 1990. Stable isotope evidence for gradual environmental changes and species survivorship across the Cretaceous/Tertiary boundary. Paleoceanography 5:867–890. https://doi.org/10.1029/PA005i006p00867.

Bednarsek, N., Tarling, G.A., Bakker, D.C.E., Fielding, S., Jones, E.M., Venables, H.J., Ward, P., Kuzirian, A., Lézé, B., Feely, R.A., Murphy, E.J., 2012. Extensive dissolution of live pteropods in the Southern Ocean. Nature Geoscience 5 (12):881–885. https://doi.org/10.1038/ngeo1635.

Begon, M., Mortimer, M., Thompson, D.J., 1996. Population Ecology: A Unified Study of Plants and Animals. Blackwell, Cambridge, UK (247 pp.).

Begon, M., Harper, J.L., Townsend, C.R., 1998. Ecology: Individuals, Populations and Communities. Blackwell Science, Boston (1068 pp.).

Berggren, W.A., Ouda, K., 2003. Upper Paleocene–lower Eocene planktonic foraminiferal biostratigraphy of the Dababiya section, Upper Nile Valley (Egypt). In: Ouda, K., Aubry, M.-P. (Eds.), The Upper Paleocene–Lower Eocene of the Upper Nile Valley: Part 1, Stratigraphy. vol. 49. Micropaleontology:pp. 61–92. https://doi.org/10.2113/49.Suppl_1.61 (supplement 1).

Bond, D.P.G., Wignall, P.B., 2014. Large igneous provinces and mass extinctions: Anupdate. In: Keller, G., Kerr, A (Eds.), volcanism, Impacts and MassExtinctions: Causes and Effects, Geological Society of America Special Papers. 505:pp. 29–55. https://doi.org/10.1130/2014.2505(02).

Borths, M.R., Ausich, W.I., 2011. Ordovician–Silurian Lilliput crinoids during the end-Ordovician biotic crisis. Swiss Journal of Palaeontology 130 (1):7–18. https://doi.org/10.1007/s13358-010-0003-2.

Bosetti, E.P., Grahn, Y., Horodyski, R.S., Mauller, P.M., Breuer, P., Zabini, C., 2010. An earliest Givetian "Lilliput Effect" in the Paraná Basin, and the collapse of the Malvinokaffric shelly fauna. Paläontologische Zeitschrift 85 (1):49–65. https://doi.org/10.1007/s12542-010-0075-8.

Bowen, G.J., Zachos, J.C., 2010. Rapid carbon sequestration at the termination of the Palaeocene-Eocene Thermal Maximum. Nature Geoscience 3:866–869. https://doi.org/10.1038/ngeo1014.

Ceballos, G., Ehrlich, P.R., 2002. Mammal population losses and the extinction crisis. Science 296:904–907. https://doi.org/10.1126/science.1069349.

Charles, A.J., Condon, D.J., Harding, I.C., Pälike, H., Marshall, J.E., Cui, Y., Kump, L., Croudace, I.W., 2011. Constraints on the numerical age of the Paleocene-Eocene boundary. Geochemistry, Geophysics, Geosystems 12 (6). https://doi.org/10.1029/2010GC003426.

Chenet, A.-L., Fluteau, F., Courtillot, V., Gérard, M., Subbarao, K.V., 2008. Determination of rapid Deccan eruptions across the Cretaceous-Tertiary boundary using paleomagnetic secular variation: results from a 1200-m-thick section in the Mahabaleshwar escarpment. Journal of Geophysical Research - Solid Earth 113 (B4). https://doi.org/10.1029/2006JB004635.

Chenet, A.-L., Courtillot, V., Fluteau, F., Gerard, M., Quidelleur, X., Khadri, S.F.R., Subbarao, K.V., Thordarson, T., 2009. Determination of rapid Deccan eruptions across the Cretaceous-Tertiary boundary using paleomagnetic secular variation: 2. Constraints from analysis of eight new sections and synthesis for a 3500-m-thick composite section. Journal of Geophysical Research 114:B06103. https://doi.org/10.1029/2008JB005644.

Chu, D., Tong, J., Song, H., Benton, M.J., Song, H., Yu, J., Qiu, X., Huang, Y., Tian, L., 2015. Lilliput effect in freshwater ostracods during the Permian–Triassic extinction. Palaeogeography, Palaeoclimatology, Palaeoecology 435:38–52. https://doi.org/10.1016/j.palaeo.2015.06.003.

Clyde, W.C., Gingerich, P.D., 1998. Mammalian community response to the latest Paleocene thermal maximum: an isotaphonomic study in the northern Bighorn Basin, Wyoming. Geology 26:1011–1014. https://doi.org/10.1130/0091-7613(1998)026<1011: MCRTTL>2.3.CO;2.

Clyde, W.C., Khan, I.H., Gingerich, P.D., 2003. Stratigraphic response and mammalian dispersal during initial India-Asia collision: evidence from the Ghazij Formation, Balochistan, Pakistan. Geology 31 (12):1097–1100. https://doi.org/10.1130/G19956.1.

Coccioni, R., Luciani, V., 2006. Guembelitria irregularis bloom at the K-T boundary: morphological abnormalities induced by impact-related extreme environmental stress? In: Cockell, C., Koeberl, C., Gilmour, I. (Eds.), Biological Processes Associated With Impact Events. Impact Studies. Berlin, Springer, pp. 179–196

Coccioni, R., Bancala, G., Catanzarit, R., Fornaciari, E., Frontalini, F., Giusberti, L., Jovane, L., Luciani, V., Savian, J., andSprovieri, M., 2012. An integrated stratigraphic record of the Palaeocene–lower Eocene at Gubbio (Italy): new insights into the early Palaeogene hyperthermals and carbon isotope excursions. Terra Nova 24 (5):380–386. https://doi.org/10.1111/j.1365-3121.2012.01076.x.

Courtillot, V., Fluteau, F., 2014. A review of the embedded time scales of flood basalt volcanism with special emphasis on dramatically short magmatic pulses. In: Keller, G., Kerr, A.C. (Eds.), Volcanism, Impacts, and Mass Extinctions: Causes and Effects. Geological Society of America Special Paper, 505:pp. 301–317 https://doi.org/10.1130/2014.2505(15).

Cowie, J.W., Ziegler, W., Remane, J., 1989. Stratigraphic commission accelerates progress, 1984 to 1989. Episodes 12, 79–83.

Culver, S.J., 2003. Benthic foraminifera across the Cretaceous–Tertiary (K–T) boundary: a review. Marine Micropaleontology 47 (3):177–226. https://doi.org/10.1016/S0377-8398(02)00117-2.

da Silva, A.C., Potma, K., Weissenberger, J.A., Whalen, M.T., Humblet, M., Mabille, C., Boulvain, F., 2009. Magnetic susceptibility evolution and sedimentary environments on carbonate platform sediments and atolls, comparison of the Frasnian from Belgium and Alberta, Canada. Sedimentary Geology 214 (1):3–18. https://doi.org/10.1016/j.sedgeo.2008.01.010.

D'Ambrosia, A.R., Clyde, W.C., Fricke, H.C., Gingerich, P.D., Abels, H.A., 2017. Repetitive mammalian dwarfing during ancient greenhouse warming events. Science Advances 3 (3), e1601430. https://doi.org/10.1126/sciadv.1601430.

Dickens, G.R., 2000. Methane oxidation during the late Palaeocene thermal maximum. Bulletin de la Société géologique de France 171 (1), 37–49.

Dickens, G.R., 2003. Rethinking the global carbon cycle with a large, dynamic and microbially mediated gas hydrate capacitor. Earth and Planetary Science Letters 213:169–183. https://doi.org/10.1016/S0012-821X(03)00325-X.

Dickens, G.R., O'Neil, J.R., Rea, D.C., Owen, R.M., 1995. Dissociation of oceanic methane hydrate as a cause of the carbon isotope excursion at the end of the Paleocene. Paleoceanography 10:965–971. https://doi.org/10.1029/95PA02087.

Dirzo, R., Raven, P.H., 2003. Global state of biodiversity and loss. Annual Review of Environment and Resources 28 (1), 137–167.

Donovan, M.P., Iglesias, A., Wilf, P., Labandeira, C.C., Cúneo, N.R., 2016. Rapid recovery of Patagonian plant–insect associations after the end-Cretaceous extinction. Nature Ecology & Evolution 1:0012. https://doi.org/10.1038/s41559-016-0012.

Dupuis, C., Aubry, M.-P., Steurbaut, E., Berggren, W.A., Ouda, K., Magioncalda, R., Cramer, B.S., Kent, D.V., Speijer, R.P., Heilmann-Clausen, C., 2003. The Dababiya Quarry section: lithostratigraphy, clay mineralogy, geochemistry and paleontology. In: Ouda, K., Aubry, M.-P. (Eds.), The Upper Paleocene–Lower Eocene of the Upper Nile Valley: Part 1. Stratigraphy. Micropaleontology vol. 49:pp. 41–59. https://doi.org/10.2113/49.Suppl_1.41.

Feduccia, A., 2014. Avian extinction at the end of the Cretaceous: assessing the magnitude and subsequent explosive radiation. Cretaceous Research 50:1–15. https://doi.org/10.1016/j.cretres.2014.03.009.

Font, E., Nédélec, A., Ellwood, B.B., Mirão, J., Silva, P.F., 2011. A new sedimentary benchmark for the Deccan Traps volcanism? Geophysical Research Letters 38 (24), L24309. https://doi.org/10.1029/2011GL049824.

Font, E., Fabre, S., Nédélec, A., Adatte, T., Keller, G., Veiga-Pires, C., Ponte, J., Mirão, J., Khozyem, H., Spangenberg, J.E., 2014. Atmospheric halogen and acid rains during the main phase of Deccan eruptions: magnetic and mineral evidence. Geological Society of America, Special Paper 505:353–368. https://doi.org/10.1130/2014.2505(18).

Font, E., Adatte, T., Sial, A.N., de Lacerda, L.D., Keller, G., Punekar, J., 2016. Mercury anomaly, Deccan volcanism, and the end-Cretaceous mass extinction. Geology 44 (2): 171–174. https://doi.org/10.1130/G37451.1.

Font, E., Adatte, T., Andrade, M., Keller, G., Bitchong, A.M Carvallo, C., Ferreira, J., DiogoZ, Mirao J., 2018. Cretaceous-Paleogene transition at Zumaia, Spain: Evidence frommagnetic, mineralogical and biostratigraphic records. Earth and PlanetaryScience Letters 484, 53–66.

Glikson, A.Y., 2014. Evolution of the Atmosphere, Fire and the Anthropocene Climate Event Horizon. Springer, Netherlands:p. 174 https://doi.org/10.1007/978-94-007-7332-5.

Gong, Q., Wang, X., Zhao, L., Grasby, S.E., Chen, Z.Q., Zhang, L., Li, Y., Cao, L., Li, Z., 2017. Mercury spikes suggest volcanic driver of the Ordovician-Silurian mass extinction. Scientific Reports 7:5304. https://doi.org/10.1038/s41598-017-05524-5.

Gradstein, F.M., Ogg, J., Smith, A., 2004. A Geologic Time Scale. Cambridge University Press, Cambridge, U.K., p. 598 (ISBN-13: 9780511074059).

Grasby, S.E., Sanei, H., Beauchamp, B., Chen, Z.H., 2013. Mercury deposition through the Permo-Triassic biotic crisis. Chemical Geology 351:209–216. https://doi.org/10.1016/j.chemgeo.2013.05.022.

Gutjahr, M., Ridgwell, A., Sexton, P.F., Anagnostou, E., Pearson, P.N., Pälike, H., Norris, R.D., Thomas, E., Foster, G.L., 2017. Very large release of mostly volcanic carbon during the

Palaeocene-Eocene Thermal Maximum. Nature 548 (7669):573–577. https://doi.org/10.1038/nature23646.

Hauri, C., Friedrich, T., Timmermann, A., 2016. Abrupt onset and prolongation of aragonite undersaturation events in the Southern Ocean. Nature Climate Change 6 (2):172–176. https://doi.org/10.1038/nclimate2844.

Hay, W.W., 2011. Can humans force a return to a 'Cretaceous' climate? Sedimentary Geology 235:5–26. https://doi.org/10.1016/j.sedgeo.2010.04.015.

Hirschmann, M.M., Renne, P.R., McBirney, A.R., 1997. $^{40}Ar/^{39}Ar$ dating of the Skaergaard intrusion. Earth and Planetary Science Letters 146:645–658. https://doi.org/10.1016/S0012-821X(96)00250-6.

Hönisch, B., Ridgwell, A., Schmidt, D.N., Thomas, E., Gibbs, S.J., Sluijs, A., Zeebe, R., Kump, L., Martindale, R.C., Greene, S.E., Kiessling, G., Ries, J., Zachos, J.C., Royer, D.L., Barker, S., Marchitto Jr., T.M., Moyer, R., Pelejero, C., Ziveri1, P., Foster, G.L., Williams, B., 2012. The geological record of ocean acidification. Science 335 (6072):1058–1063. https://doi.org/10.1126/science.1208277.

Hooker, J.J., 1998. Mammalian faunal change across the Paleocene-Eocene transition in Europe. In: Aubry, M.P., Lucas, S., Berggren, W.A. (Eds.), Late Paleocene-Early Eocene Climatic and Biotic Events in the Marine and Terrestrial Records. Columbia University Press, New York, pp. 428–450.

Hughes, J.B., Daily, G.C., Ehrlich, P.R., 1997. Population diversity: its extent and extinction. Science 278:689–692. https://doi.org/10.1126/science.278.5338.689.

Hunt, B.P.V., Pakhomov, E.A., Hosie, G.W., Siegel, V., Ward, P., Bernard, K., 2008. Pteropods in southern ocean ecosystems. Progress in Oceanography 78 (3):193–221. https://doi.org/10.1016/j.pocean.2008.06.001.

IPCC, 2007. Climate change 2007: the physical science basis. In: Solomon, S., Qin, D., Manning, M., Chen, Z., Marquis, M., Averyt, K.B., Tignor, M., Miller, H.L. (Eds.), Contribution of Working Group I to the Fourth Assessment Report of the Intergovernmental Panel on Climate Change. Cambridge University Press, Cambridge, United Kingdom and New York, NY, USA.

IPCC, 2013. Climate change 2013: the physical science basis. In: Stocker, T.F., Qin, D., Plattner, G.-K., Tignor, M., Allen, S.K., Boschung, J., Nauels, A., Xia, Y., Bex, V., Midgley, P.M. (Eds.), Contribution of Working Group I to the Fifth Assessment Report of the Intergovernmental Panel on Climate Change. Cambridge University Press, Cambridge, United Kingdom and New York, NY, USA.

Kaiho, K., Takeda, K., Petrizzo, M.R., Zachos, J.C., 2006. Anomalous shifts in tropical Pacific planktonic and benthic foraminiferal test size during the Paleocene–Eocene thermal maximum. Palaeogeography, Palaeoclimatology, Palaeoecology 237 (2):456–464. https://doi.org/10.1016/j.palaeo.2005.12.017.

Keller, G., 1988a. Extinction, survivorship and evolution of planktic foraminifers across the Cretaceous/Tertiary boundary at El Kef, Tunisia. Marine Micropaleontology 13: 239–263. https://doi.org/10.1016/0377-8398(88)90005-9.

Keller, G., 1988b. Biotic turnover in benthic foraminifera across the Cretaceous/Tertiary boundary at El Kef, Tunisia. Palaeogeography, Palaeoclimatology, Palaeoecology 66 (3–4):153–171. https://doi.org/10.1016/0031-0182(88)90198-8.

Keller, G., 2001. The end-cretaceous mass extinction in the marine realm: year 2000 assessment. Planetary and Space Science 49 (8):817–830. https://doi.org/10.1016/S0032-0633(01)00032-0.

Keller, G., 2003. Biotic effects of impacts and volcanism. Earth and Planetary Science Letters 215:249–264. https://doi.org/10.1016/S0012-821X(03)00390-X.

Keller, G., 2011. Defining the Cretaceous-Tertiary boundary: a practical guide and return to first principles. In: Keller, G., Adatte, T. (Eds.), The KT Mass Extinction and the Chicxulub Impact in Texas. vol. 100. SEPM Special Publication, pp. 23–42.

Keller, G., 2014. Deccan volcanism, the Chicxulub impact, and the end-Cretaceous mass extinction: coincidence? Cause and effect? In: Keller, G., Kerr, A. (Eds.), Volcanism, Impacts and Mass Extinctions: Causes and Effects. Geological Society of America Special Papers, 505:pp. 57–89 https://doi.org/10.1130/2014.2505(03)

Keller, G., Abramovich, S., 2009. Lilliput effect in late Maastrichtian planktic foraminifera: response to environmental stress. Palaeogeography, Palaeoclimatology, Palaeoecology 284:47–62. https://doi.org/10.1016/j.palaeo.2009.08.029.

Keller, G., Lindinger, M., 1989. Stable isotope, TOC and CaCO$_3$ record across the Cretaceous/Tertiary boundary at El Kef, Tunisia. Palaeogeography, Palaeoclimatology, Palaeoecology 73 (3–4):243–265. https://doi.org/10.1016/0031-0182(89)90007-2.

Keller, G., Li, L., MacLeod, N., 1995. The Cretaceous-Tertiary boundary stratotype section at El Kef, Tunisia: how catastrophic was the mass extinction? Palaeogeography, Palaeoclimatology, Palaeoecology 119:221–254. https://doi.org/10.1016/0031-0182(95)00009-7.

Keller, G., Adatte, T., Stinnesbeck, W., Luciani, V., Karoui-Yaakoub, N., Zaghbib-Turki, D., 2002. Paleoecology of the Cretaceous–Tertiary mass extinction in planktonic foraminifera. Palaeogeography, Palaeoclimatology, Palaeoecology 178 (3):257–297. https://doi.org/10.1016/S0031-0182(01)00399-6.

Keller, G., Adatte, T., Tantawy, A.A., Berner, Z., Stüben, D., 2007. High stress late Cretaceous to early Danian paleoenvironment in the Neuquen Basin, Argentina. Cretaceous Research 28:939–960. https://doi.org/10.1016/j.cretres.2007.01.006.

Keller, G., Adatte, T., Gardin, S., Bartolini, A., Bajpai, S., 2008. Main Deccan volcanism phase ends near the K-T boundary: evidence from the Krishna-Godavari Basin, SE India. Earth and Planetary Science Letters 268:293–311. https://doi.org/10.1016/j.epsl.2008.01.015.

Keller, G., Adatte, T., Pardo, A., Lopez-Oliva, J.G., 2009. New evidence concerning the age and biotic effects of the Chicxulub impact in NE Mexico. Journal of the Geological Society of London 166 (3):393–411. https://doi.org/10.1144/0016-76492008-116.

Keller, G., Bhowmick, P.K., Upadhyay, H., Dave, A., Reddy, A.N., Jaiprakash, B.C., Adatte, T., 2011a. Deccan volcanism linked to the Cretaceous-Tertiary boundary (KTB) mass extinction: new evidence from ONGC wells in the Krishna-Godavari Basin, India. Journal of the Geological Society of India 78:399–428. https://doi.org/10.1007/s12594-011-0107-3.

Keller, G., Abramovich, S., Adatte, T., Berner, Z., 2011b. Biostratigraphy, Age of the Chicxulub impact, and depositional environment of the Brazos River KTB sequences.

In: Keller, G., Adatte, T. (Eds.), The End-Cretaceous Mass Extinction and the Chicxulub Impact in Texas. Society for Sedimentary Geology Special Publication 100:pp. 81–122 https://doi.org/10.2110/sepmsp.100.081.

Keller, G., Adatte, T., Bhowmick, P.K., Upadhyay, H., Dave, A., Reddy, A.N., Jaiprakash, B.C., 2012. Nature and timing of extinctions in Cretaceous–Tertiary planktic foraminifera preserved in Deccan intertrappean sediments of the Krishna-Godavari Basin, India. Earth and Planetary Science Letters 341:211–221. https://doi.org/10.1016/j.epsl.2012.06.021.

Keller, G., Khozyem, H.M., Adatte, T., Malarkodi, N., Spangenberg, J.E., Stinnesbeck, W., 2013. Chicxulub impact spherules in the North Atlantic and Caribbean: age constraints and Cretaceous-Tertiary boundary hiatus. Geological Magazine 150: 885–907. https://doi.org/10.1017/S0016756812001069.

Keller, G., Punekar, J., Mateo, P., 2016. Upheavals during the late Maastrichtian: volcanism, climate and faunal events preceding the end-Cretaceous mass extinction. Palaeogeography, Palaeoclimatology, Palaeoecology 441:137–151. https://doi.org/10.1016/j.palaeo.2015.06.034.

Kelly, D.C., Bralower, T.J., Zachos, J.C., Premoli-Silva, I., Thomas, E., 1996. Rapid diversification of planktonic foraminifera in the tropical Pacific (ODP Site 865) during the late Paleocene Thermal Maximum. Geology 24:423–426. https://doi.org/10.1130/0091-7613(1996)024<0423:RDOPFI>2.3.CO;2.

Kelly, D.C., Bralower, T.J., Zachos, J.C., 1998. Evolutionary consequences of the latest Paleocene thermal maximum for tropical planktonic foraminifera. Palaeogeography, Palaeoclimatology, Palaeoecology 141:139–161. https://doi.org/10.1016/S0031-0182(98)00017-0.

Kennett, J.P., Stott, L.D., 1991. Abrupt deep-sea warming, palaeoceanographic changes and benthic extinctions at the end of the Palaeocene. Nature 353, 225–229.

Khozyem, H., Adatte, T., Keller, G., Tantawy, A.A., Spangenberg, J.E., 2014. The Paleocene-Eocene GSSP at Dababiya, Egypt-revisited. Episodes 37 (2), 78–86.

Khozyem, H., Adatte, T., Spangenberg, J.E., Keller, G., Tantawy, A.A., Ulianov, A., 2015. New geochemical constraints on the Paleocene–Eocene thermal maximum: Dababiya GSSP, Egypt. Palaeogeography, Palaeoclimatology, Palaeoecology 429:117–135. https://doi.org/10.1016/j.palaeo.2015.04.003.

Khozyem, H., Adatte, T., Bitchong, A., Mohamed, A., Keller, G., 2017. The role of volcanism (North Atlantic Igneous Province) in the PETM events revealed by Mercury anomalies. Geological Society of AMerica Abstracts with Programs 49 (6). https://doi.org/10.1130/abs/2017AM-302839.

Koch, P.L., Zachos, J.C., Gingerich, P.D., 1992. Correlation between isotope records in marine and continental carbon reservoirs near the Palaeocene/Eocene boundary. Nature 358 (6384):319–322. https://doi.org/10.1002/palo.20016.

Koch, P.L., Zachos, J.C., Dettman, D.L., 1995. Stable isotope stratigraphy and paleoclimatology of the Paleogene Bighorn Basin (Wyoming, USA). Palaeogeography, Palaeoclimatology, Palaeoecology 115 (1–4):61–89. https://doi.org/10.1016/0031-0182(94)00107-J.

Kump, L.R., 1991. Interpreting carbon-isotope excursions: strangelove oceans. Geology 19:299–302. https://doi.org/10.1130/0091-7613(1991)019<0299:ICIESO>2.3.CO;2.

Kump, L.R., 2003. The geochemistry of mass extinction. In: Mackenzie, F.T. (Ed.), Treatise on Geochemistry. vol. 7. Elsevier:pp. 351–367. https://doi.org/10.1016/B0-08-043751-6/07101-2.

Kump, L., Bralower, T., Ridgwell, A., 2009. Ocean acidification in deep time. Oceanography 22 (4), 94–107.

Labandeira, C.C., Johnson, K.R., Lang, P., 2002. Preliminary assessment of insect herbivory across the Cretaceous-Tertiary boundary: major extinction and minimum rebound. Geological Society of America, Special Paper 361, 297–327.

Le Quéré, C., Andres, R.J., Boden, T., Conway, T., Houghton, R.A., House, J.I., Marland, G., Peters, G.P., Van der Werf, G.R., Ahlström, A., Andrew, R.M., 2013. The global carbon budget 1959–2011. Earth System Science Data 5 (1):165–185. https://doi.org/10.5194/essd-5-165-2013.

Leakey, R., Lewin, R., 1992. The Sixth Extinction: Patterns of Life and the Future of Humankind. Anchor Books, p. 271.

Li, L., Keller, G., 1998. Abrupt deep-sea warming at the end of the Cretaceous. Geology 26: 995–998. https://doi.org/10.1130/0091-7613(1998)026<0995:ADSWAT>2.3.CO;2.

Longrich, N.R., Tokaryk, T., Field, D.J., 2011. Mass extinction of birds at the Cretaceous-Paleogene (K–Pg) boundary. Proceedings of the National Academy of Sciences 108 (37):15253–15257. https://doi.org/10.1073/pnas.1110395108.

Longrich, N.R., Bhullar, B.A.S., Gauthier, J.A., 2012. Mass extinction of lizards and snakes at the Cretaceous–Paleogene boundary. Proceedings of the National Academy of Sciences 109 (52):21396–21401. https://doi.org/10.1073/pnas.1211526110.

Lu, G., Keller, G., 1993. Climatic and oceanographic events across the Paleocene-Eocene Transition in the Antarctic Indian Ocean: inference from planktic foraminifera. Marine Micropaleontology 21, 101–142.

Lu, G., Keller, G., 1995a. Ecological stasis and saltation: species richness change in planktic foraminifera during the late Paleocene to early Eocene, DSDP Site 577. Palaeogeography, Palaeoclimatology, Palaeoecology 117:211–227. https://doi.org/10.1016/0031-0182(94)00125-R.

Lu, G., Keller, G., 1995b. Planktic foraminiferal turnovers in the subtropical Pacific during the late Paleocene to early Eocene. Journal of Foraminiferal Research 25, 97–116.

Lu, G., Keller, G., Adatte, T., Ortiz, N., Molina, E., 1996. Long-term (10^5) or short-term (10^3) $\delta^{13}C$ excursion near the Paleocene-Eocene transition: evidence from the Tethys. Terra Nova 8, 347–355.

Lu, G., Adatte, T., Keller, G., Ortiz, S., 1998. Abrupt climatic, oceanographic and ecologic changes near the Paleocene-Eocene transition in the deep Tethys basin: the Alamedilla section, southern Spain. Eclogae Geologicae Helvetiae 91, 293–306.

Luciani, V., 2002. High-resolution planktonic foraminiferal analysis from the Cretaceous–Tertiary boundary at Ain Settara (Tunisia): evidence of an extended mass extinction. Palaeogeography, Palaeoclimatology, Palaeoecology 178 (3):299–319. https://doi.org/10.1016/S0031-0182(01)00400-X.

Luciani, V., Giusberti, L., Agnini, C., Backman, J., Fornaciari, E., Rio, D., 2007. The Paleocene-Eocene Thermal Maximum as recorded by Tethyan planktonic foraminifera in the Forada section (northern Italy). Marine Micropaleontology 64 (3):189–214. https://doi.org/10.1016/j.marmicro.2007.05.001.

Luciani, V., Dickens, G.R., Backman, J., Fornaciari, E., Giusberti, L., Agnini, C., D'Onofrio, R., 2016. Major perturbations in the global carbon cycle and photosymbiont-bearing planktic foraminifera during the early Eocene. Climate of the Past 12:981–1007. https://doi.org/10.5194/cp-12-981-2016.

Maclennan, J., Jones, S.M., 2006. Regional uplift, gas-hydrate dissociation and the origins of the Paleocene–Eocene Thermal Maximum. Earth and Planetary Science Letters 245 (1):65–80. https://doi.org/10.1016/j.epsl.2006.01.069.

MacLeod, N., Rawson, P.F., Forey, P.L., Banner, F.T., Boudagher-Fadel, M.K., Bown, P.R., Burnett, J.A., Chambers, P., Culver, S., Evans, S.E., Jeffery, C., Kaminski, M.A., Lord, A.R., Milner, A.C., Milner, A.R., Morris, N., Owen, E., Rosen, B.R., Smith, A.B., Taylor, P.D., Urquhart, E., Young, J.R., 1997. The Cretaceous-Tertiary biotic transition. Journal of the Geological Society 154 (2):265–292. https://doi.org/10.1144/gsjgs.154.2.0265.

Mateo, P., Keller, G., Punekar, J., Spangenberg, J.E., 2017. Early to Late Maastrichtian environmental changes in the Indian Ocean compared with Tethys and South Atlantic. Palaeogeography, Palaeoclimatology, Palaeoecology 478:121–138. https://doi.org/10.1016/j.palaeo.2017.01.027.

May, R.M., Lawton, J.H., Stork, N.E., 1995. Assessing extinction rates. Extinction Rates, pp. 1–24.

McInerney, F.A., Wing, S.L., 2011. The Paleocene-Eocene Thermal Maximum: a perturbation of carbon cycle, climate, and biosphere with implications for the future. Annual Review of Earth and Planetary Sciences 39:489–516. https://doi.org/10.1146/annurev-earth-040610-133431.

McNeil, B.I., Matear, R.J., 2008. Southern Ocean acidification: a tipping point at 450-ppm atmospheric CO_2. Proceedings of the National Academy of Sciences 105 (48): 18860–18864. https://doi.org/10.1073/pnas.0806318105.

Molina, E., Arenillas, I., Arz, J.A., 1998. Mass extinction in planktic foraminifera at the Cretaceous/Tertiary boundary in subtropical and temperate latitudes. Bulletin de la Société géologique de France 169 (3), 351–363.

Molina, E., Alegret, L., Arenillas, I., Arz, J.A., Gallala, N., Hardenbol, J., von Salis, K., Steurbaut, E., Vandenberghe, N., Zaghbib-Turki, D., 2006. The global boundary stratotype section and point for the base of the Danian stage (Paleocene, Paleogene, "Tertiary", Cenozoic) at El Kef, Tunisia: original definition and revision. Episodes 29 (4), 263–273.

Molina, E., Alegret, L., Arenillas, I., Arz, J.A., Gallala, N., Grajales-Nishimura, J.M., Murillo-Muneton, G., Zaghbib-Turki, D., 2009. The global boundary stratotype section and point for the base of the Danian stage (Paleocene, Paleogene, "Tertiary", Cenozoic): auxiliary sections and correlation. Episodes 32 (2), 84–95.

Nichols, D.J., Johnson, K.R., 2008. Plants and the KT Boundary. Cambridge University Press, New York, p. 279.

Nordt, L, Atchley, S., Dworkin, S., 2003. Terrestrial evidence for two greenhouse events in the Latest Cretaceous. GSA Today 13, 4–9.

Olsson, R.K., Hemleben, C., Berggren, W.A., Huber, B.T., 1999. Atlas of Paleocene planktic foraminifera. Smithsonian Contributions to Paleobiology. vol. 85. Smithsonian Institution Press, Washington, DC, p. 252.

Olsson, R.K., Wright, J.D., Miller, K.G., 2001. Paleobiogeography of Pseudotextularia elegans during the latest Maastrichtian global warming event. Journal of Foraminiferal Research 31:275–282. https://doi.org/10.2113/31.3.275.

Panchuk, K., Ridgwell, A., Kump, L.R., 2008. Sedimentary response to Paleocene-Eocene Thermal Maximum carbon release: a model-data comparison. Geology 36 (4): 315–318. https://doi.org/10.1130/G24474A.1.

Pardo, A., Keller, G., 2008. Biotic effects of environmental catastrophes at the end of the Cretaceous: Guembelitria and Heterohelix blooms. Cretaceous Research 29 (5–6): 1058–1073. https://doi.org/10.1016/j.cretres.2008.05.031.

Pardo, A., Ortiz, N., Keller, G., 1996. Latest Maastrichtian and K/T boundary foraminiferal turnover and environmental changes at Agost, Spain. In: MacLeod, N., Keller, G. (Eds.), The Cretaceous-Tertiary Mass Extinction: Biotic and Environmental Effects. Norton Press, New York, pp. 157–191.

Pardo, A., Keller, G., Oberhaensli, H., 1999. Paleoecologic and paleoceanographic evolution of the Tethyan realm during the Paleocene-Eocene transition. Journal of Foraminiferal Research 29 (1), 37–57.

Payne, J.L., 2005. Evolutionary dynamics of gastropod size across the end-Permian extinction and through the Triassic recovery interval. Paleobiology 31 (2):269–290. https://doi.org/10.1666/0094-8373(2005)031[0269:EDOGSA]2.0.CO;2.

Pearson, P.N., Olsson, R.K., Huber, B.T., Hemleben, C., Berggren, W.A., 2006. Atlas of Eocene planktonic foraminifera 41. Cushman Foundation Special Publication, pp. 1–513.

Penman, D.E., Hönisch, B., Zeebe, R.E., Thomas, E., Zachos, J.C., 2014. Rapid and sustained surface ocean acidification during the Paleocene-Eocene Thermal Maximum. Paleoceanography 29 (5):357–369. https://doi.org/10.1002/2014PA002621.

Percival, L.M.E., Witt, M.L.I., Mather, T.A., Hermoso, M., Jenkyns, H.C., Hesselbo, S.P., Al-Suwaidi, A.H., Storm, M.S., Xu, W., Ruhl, M., 2015. Globally enhanced mercury deposition during the end-Pliensbachian extinction and Toarcian OAE: a link to the Karoo–Ferrar large igneous province. Earth and Planetary Science Letters 428:267–280. https://doi.org/10.1016/j.epsl.2015.06.064.

Pereira, H.M., Leadley, P.W., Proença, V., Alkemade, R., Scharlemann, J.P., Fernandez-Manjarrés, J.F., Araújo, M.B., Balvanera, P., Biggs, R., Cheung, W.W., Chini, L., 2010. Scenarios for global biodiversity in the 21st century. Science 330 (6010):1496–1501. https://doi.org/10.1126/science.1196624.

Punekar, J., Saraswati, P.K., 2010. Age of the Vastan lignite in context of some oldest Cenozoic fossil mammals from India. Journal of the Geological Society of India 76 (1): 63–68. https://doi.org/10.1007/s12594-010-0076-y.

Punekar, J., Mateo, P., Keller, G., 2014. Effects of Deccan volcanism on paleoenvironment and planktic foraminifera: a global survey. Geological Society of America Special Papers 505:91–116. https://doi.org/10.1130/2014.2505(04.

Punekar, J., Keller, G., Khozyem, H.M., Adatte, T., Font, E., Spangenberg, J., 2016. A multi-proxy approach to decode the end-Cretaceous mass extinction. Palaeogeography, Palaeoclimatology, Palaeoecology 441:116–136. https://doi.org/10.1016/j.palaeo.2015.08.025.

Remane, J., Keller, G., Hardenbol, J., Ben Haj Ali, M., 1999. Report on the International Workshop on Cretaceous-Paleogene Transitions. Episodes 22, 47–48.

Renne, P.R., Sprain, C.J., Richards, M.A., Self, S., Vanderkluysen, L., Pande, K., 2015. State shift in Deccan volcanism at the Cretaceous-Paleogene boundary, possibly induced by impact. Science 350 (6256):76–78. https://doi.org/10.1126/science.aac7549.

Richards, M.A., Alvarez, W., Self, S., Karlstrom, L., Renne, P.R., Manga, M., Sprain, C.J., Smit, J., Vanderkluysen, L., Gibson, S.A., 2015. Triggering of the largest Deccan eruptions by the Chicxulub impact. Geological Society of America Bulletin 127 (11 − 12): 1507–1520. https://doi.org/10.1130/B31167.1.

Rose, K.D., DeLeon, V.B., Missiaen, P., Rana, R.S., Sahni, A., Singh, L., Smith, T., 2008. Early Eocene lagomorph (Mammalia) from Western India and the early diversification of Lagomorpha. Proceedings of the Royal Society of London B: Biological Sciences 275 (1639):1203–1208. https://doi.org/10.1098/rspb.2007.1661.

Schoene, B., Samperton, K.M., Eddy, M.P., Keller, G., Adatte, T., Bowring, S.A., Khadri, S.F.R., Gertsch, B., 2015. U–Pb geochronology of the Deccan Traps and relation to the end-Cretaceous mass extinction. Science 347:182–184. https://doi.org/10.1126/science.aaa0118.

Schulte, P., Alegret, L., Arenillas, I., Arz, J.A., Barton, P.J., Bown, P.R., Bralower, T.J., Christeson, G.L., Claeys, P., Cockell, C.S., Collins, G.S., Deutsch, A., Goldin, T.J., Goto, K., Grajales-Nishimura, J.M., Grieve, R.A.F., Gulick, S.P.S., Johnson, K.R., Kiessling, W., Koeberl, C., Kring, D.A., MacLeod, K.G., Matsui, T., Melosh, J., Montanari, A., Morgan, J.V., Neal, C.R., Nichols, D.J., Norris, R.D., Pierazzo, E., Ravizza, G., Rebolledo-Vieyra, M., Reimold, W.U., Robin, E., Salge, T., Speijer, R.P., Sweet, A.R., Urrutia-Fucugauchi, J., Vajda, V., Whalen, M.T., Willumsen, P.S., 2010. The Chicxulub asteroid impact and mass extinction at the Cretaceous-Paleogene boundary. Science 327:1214–1218. https://doi.org/10.1126/science.1177265.

Schulte, P., Scheibner, C., Speijer, R., 2011. Fluvial discharge and sea-level changes controlling black shale deposition during the Paleocene–Eocene Thermal Maximum in the Dababiya Quarry section, Egypt. Chemical Geology 285:167–183. https://doi.org/10.1016/j.chemgeo.2011.04.004.

Scotese, C.R., 2013a. Map folio 16, KT boundary (65.5 Ma, latest Maastrichtian), PALEOMAP PaleoAtlas for ArcGIS. Cretaceous. vol. 2. PALEOMAP Project, Evanston, IL. https://doi.org/10.13140/2.1.3498.1129.

Scotese, C.R., 2013b. Map folio 14, PETM (55.8 Ma, Thanetian/Ypresian boundary), PALEOMAP PaleoAtlas for ArcGIS. Cenozoic. vol. 1. PALEOMAP Project, Evanston, IL. https://doi.org/10.13140/2.1.2388.0961.

Self, S., Jay, A.E., Widdowson, M., Keszthelyi, L.P., 2008. Correlation of the Deccan and Rajahmundry Trap lavas: are these the longest and largest lava flows on Earth? Journal of Volcanology and Geothermal Research 172:3–19. https://doi.org/10.1016/j.jvolgeores.2006.11.012.

Self, S., Schmidt, A., Mather, T.A., 2014. Emplacement characteristics, time scales, and volcanic gas release rates of continental flood basalt eruptions on Earth. In: Keller, G., Kerr, A.C. (Eds.), Volcanism, Impacts, and Mass Extinctions: Causes and Effects. Geological Society of America Special Paper 505:pp. 319–337 https://doi.org/10.1130/2014.2505(16.

Sigurdsson, H., Leckie, R.M., Acton, G., 1997. Proceedings of the Ocean Drilling Program, Initial Reports. vol. 165. Ocean Drilling Program, College Station, Texas (865 pp.).

Silva, M.V.N., Sial, N.A., Barbosa, J.A., Ferreira, V.P., Neumann, V.H., de Lacerca, L.D., 2013. Carbon isotopes, rare-earth elements and mercury geochemistry across the K-T transition of the Paraíba Basin, northeastern Brazil. Geological Society of London, Special Publication 382:85–104. https://doi.org/10.1144/SP382.2.

Sinton, C.W., Duncan, R.A., 1998. ^{40}Ar-^{39}Ar ages of lavas from the Southeast Greenland margin, ODP Leg 152, and the Rockall Plateau, DSDP Leg 81. Proceedings of the Ocean Drilling Program, Scientific Results. vol. 152:pp. 387–402. https://doi.org/10.2973/odp.proc.sr.152.234.1998.

Sluijs, A., Schouten, S., Pagani, M., Woltering, M., Brinkhuis, H., Damsté, J.S.S., Dickens, G.R., Huber, M., Reichart, G.-J., Stein, R., Matthiessen, J., Lourens, L.J., Pedentchouk, N., Backman, J., Moran, K., the Expedition 302 Scientists, 2006. Subtropical Arctic Ocean temperatures during the Palaeocene/Eocene thermal maximum. Nature 441 (7093):610–613. https://doi.org/10.1038/nature04668.

Sluijs, A., Brinkhuis, H., Crouch, E.M., John, C.M., Handley, L., Munsterman, D., Bohaty, S.M., Zachos, J.C., Reichart, G.-J., Schouten, S., Pancost, R.D., Sinninghe Damste, J.S., 2008. Eustatic variations in the Paleocene–Eocene greenhouse world. Paleoceanography 23, PA4216. https://doi.org/10.1029/2008PA001615.

Smith, F.A., 2012. Some like it hot. Science 335 (6071):924–925. https://doi.org/10.1126/science.1219233.

Smith, T., Rose, K.D., Gingerich, P.D., 2006. Rapid Asia–Europe–North America geographic dispersal of earliest Eocene primate Teilhardina during the Paleocene–Eocene thermal maximum. Proceedings of the National Academy of Sciences 103 (30): 11223–11227. https://doi.org/10.1073/pnas.0511296103.

Smith, J.J., Hasiotis, S.T., Kraus, M.J., Woody, D.T., 2009. Transient dwarfism of soil fauna during the Paleocene–Eocene Thermal Maximum. Proceedings of the National Academy of Sciences 106 (42):17655–17660. https://doi.org/10.1073/pnas.0909674106.

Soliman, M.F., Ahmed, E., Kurzweil, H., 2006. Geochemistry and mineralogy of the Paleocene/Eocene boundary at Gabal Dababiya (GSSP) and Gabal Owaina sections, Nile Valley, Egypt. Stratigraphy 3, 31–52.

Speijer, R.P., Schmitz, B., 1998. A benthic foraminiferal record of Paleocene sea level and trophic/redox conditions at Gebel Aweina, Egypt. Palaeogeography, Palaeoclimatology, Palaeoecology 137:79–101. https://doi.org/10.1016/S0031-0182(97)00107-7.

Speijer, R.P., Van der Zwaan, G.J., 1996. Extinction and survivorship of southern Tethyan benthic foraminifera across the Cretaceous/Palaeogene boundary. Geological Society

of London, Special Publication 102 (1):343–371. https://doi.org/10.1144/GSL.SP.1996.001.01.26.

Speijer, R.P., Wagner, T., 2002. Sea-level changes and black shales associated with the late Paleocene thermal maximum: organic-geochemical and micropaleontologic evidence from the southern Tethyan margin (Egypt-Israel). Geological Society of America, Special Paper 356, 533–549.

Speijer, R.P., Schmitz, B., Aubry, M.P., Charisi, S.D., 1995. The latest Paleocene benthic extinction event: punctuated turnover in outer neritic foraminiferal faunas from Gebel Aweina, Egypt. Israel Journal of Earth Sciences 44, 207–222.

Storey, M., Duncan, R.A., Swisher, C.C., 2007. Paleocene-Eocene Thermal Maximum and the opening of the northeast Atlantic. Science 316:587. https://doi.org/10.1126/science.1135274.

Stüben, D., Kramar, U., Berner, Z.A., Meudt, M., Keller, G., Abramovich, S., Adatte, T., Hambach, U., Stinnesbeck, W., 2003. Late Maastrichtian paleoclimatic and paleoceanographic changes inferred from Sr/Ca ratio and stable isotopes. Paleoclimatology, Paleoecology, Paleogeography 199:107–127. https://doi.org/10.1016/S0031-0182(03)00499-1.

Sunday, J.M., Calosi, P., Dupont, S., Munday, P.L., Stillman, J.H., Reusch, T.B., 2014. Evolution in an acidifying ocean. Trends in Ecology & Evolution 29 (2):117–125. https://doi.org/10.1016/j.tree.2013.11.001.

Svensen, Henrik, Planke, Sverre, Malthe-Sørenssen, Anders, Jamtveit, Bjørn, Myklebust, Reidun, Eidem, Torfinn Rasmussen, Rey, Sebastian S., 2004. Release of methane from a volcanic basin as a mechanism for initial Eocene global warming. Nature 429 (6991):542–545. https://doi.org/10.1038/nature02566.

Svensen, H., Planke, S., Corfu, F., 2010. Zircon dating ties NE Atlantic sill emplacement to initial Eocene global warming. Journal of the Geological Society of London 167: 433–436. https://doi.org/10.1144/0016-76492009-125.

Thibault, N., Husson, D., 2016. Climatic fluctuations and sea-surface water circulation patterns at the end of the Cretaceous era: Calcareous nannofossil evidence. Palaeogeography, Palaeoclimatology, Palaeoecology 441:152–164. https://doi.org/10.1016/j.palaeo.2015.07.049.

Thibault, N., Galbrun, B., Gardin, S., Minoletti, F., Le Callonec, L., 2016. The end-Cretaceous in the southwestern Tethys (Elles, Tunisia): orbital calibration of paleoenvironmental events before the mass extinction. International Journal of Earth Sciences:1–25 https://doi.org/10.1007/s00531-015-1192-0.

Thibodeau, A.M., Bergquist, B.A., 2017. Do mercury isotopes record the signature of massive volcanism in marine sedimentary records? Geology 45 (1):95–96. https://doi.org/10.1130/focus012017.1.

Thibodeau, A.M., Ritterbush, K., Yager, J.A., West, A.J., Ibarra, Y., Bottjer, D.J., Berelson, W.M., Bergquist, B.A., Corsetti, F.A., 2016. Mercury anomalies and the timing of biotic recovery following the end-Triassic mass extinction. Nature Communications 7. https://doi.org/10.1038/ncomms11147.

Thomas, E., 1998. The biogeography of the late Paleocene benthic foraminiferal extinction. In: Aubry, M.-P., Lucas, S., Berggren, W.A. (Eds.), Late Paleocene–Early Eocene Biotic and Climatic Events in the Marine and Terrestrial Records. University Press, Columbia, pp. 214–243.

Tong, Y., Wang, J., 2006. Fossil mammals from the early Eocene Wutu formation of Shandong province. Palaeontologia Sinica, New Series C 28, 1–195.

Twitchett, R.J., 2007. The Lilliput effect in the aftermath of the end-Permian extinction event. Palaeogeography, Palaeoclimatology, Palaeoecology 252 (1):132–144. https://doi.org/10.1016/j.palaeo.2006.11.038.

Urbanek, A., 1993. Biotic crises in the history of Upper Silurian graptoloids: a palaeobiological model. Historical Biology 7, 29–50.

Vajda, V., Bercovici, A., 2014. The global vegetation pattern across the Cretaceous–Paleogene mass extinction interval: a template for other extinction events. Global and Planetary Change 122:29–49. https://doi.org/10.1016/j.gloplacha.2014.07.014.

Wake, D.B., Vredenburg, V.T., 2008. Are we in the midst of the sixth mass extinction? A view from the world of amphibians. Proceedings of the National Academy of Sciences 105 (1), 11466–11473.

Weijers, J.W., Schouten, S., Sluijs, A., Brinkhuis, H., Damsté, J.S.S., 2007. Warm arctic continents during the Palaeocene–Eocene thermal maximum. Earth and Planetary Science Letters 261 (1):230–238. https://doi.org/10.1016/j.epsl.2007.06.033.

Westerhold, T., Röhl, U., McCarren, H.K., Zachos, J.C., 2009. Latest on the absolute age of the Paleocene–Eocene Thermal Maximum (PETM): new insights from exact stratigraphic position of key ash layers + 19 and − 17. Earth and Planetary Science Letters 287 (3):412–419. https://doi.org/10.1016/j.epsl.2009.08.027.

Westerhold, T., Röhl, U., Donner, B., McCarren, H.K., Zachos, J.C., 2011. A complete high-resolution Paleocene benthic stable isotope record for the central Pacific (ODP Site 1209). Paleoceanography 26, PA2216. https://doi.org/10.1029/2010PA002092.

Whalen, M.T., Day, J., Eberli, G.P., Homewood, P.W., 2002. Microbial carbonates as indicators of environmental change and biotic crisis in carbonate systems: examples from the Late Devonian, Alberta Basin, Canada. Palaeogeography, Palaeoclimatology, Palaeoecology 181, 127–151.

Wieczorek, R., Fantle, M.S., Kump, L.R., Ravizza, G., 2013. Geochemical evidence for volcanic activity prior to and enhanced terrestrial weathering during the Paleocene Eocene Thermal Maximum. Geochimica et Cosmochimica Acta 119:391–410. https://doi.org/10.1016/j.gca.2013.06.005.

Wilf, P., Johnson, K.R., 2004. Land plant extinction at the end of the Cretaceous: a quantitative analysis of the North Dakota megafloral record. Paleobiology 30 (3):347–368. https://doi.org/10.1666/0094-8373(2004)030<0347:LPEATE>2.0.CO;2.

Wilf, P., Johnson, K.R., Huber, B.T., 2003. Correlated terrestrial and marine evidence for global climate changes before mass extinction at the Cretaceous-Paleogene boundary. Proceedings of the National Academy of Sciences of the United States of America 100 (2):599–604. https://doi.org/10.1073/pnas.0234701100.

Wilson, G.P., 2005. Mammalian faunal dynamics during the last 1.8 million years of the Cretaceous in Garfield County, Montana. Journal of Mammalian Evolution 12 (1–2): 53–76. https://doi.org/10.1007/s10914-005-6943-4.

Wilson, G.P., 2014. Mammalian extinction, survival, and recovery dynamics across the Cretaceous-Paleogene boundary in northeastern Montana, USA. Geological Society of America Special Papers 503:365–392. https://doi.org/10.1130/2014.2503(15.

Wilson, G.P., DeMar, D.G., Carter, G., 2014. Extinction and survival of salamander and salamander-like amphibians across the Cretaceous-Paleogene boundary in northeastern Montana, USA. Geological Society of America Special Papers 503:271–297. https://doi.org/10.1130/2014.2503(10.

Zachos, J., Arthur, M., Dean, W., 1989. Geochemical evidence for suppression of pelagic marine productivity at the Cretaceous/Tertiary boundary. Nature 337:61–64. https://doi.org/10.1038/337061a0.

Zachos, J.C., Wara, M.W., Bohaty, S., Delaney, M.L., Petrizzo, M.R., Brill, A., Bralower, T.J., Premoli Silva, I., 2003. A transient rise in tropical sea surface temperature during the Paleocene–Eocene Thermal Maximum. Science 302:1551–1554. https://doi.org/10.1126/science.1090110.

Zachos, J.C., Röhl, U., Schellenberg, S.A., Sluijs, A., Hodell, D.A., Kelly, D.C., Thomas, E., Nicolo, M., Raffi, I., Lourens, L.J., McCarren, H., Kroon, D., 2005. Rapid acidification of the ocean during the Paleocene–Eocene Thermal Maximum. Science 308: 1611–1615. https://doi.org/10.1126/science.1109004.

Zachos, J.C., Schouten, S., Bohaty, S., Quattlebaum, T., Sluijs, A., Brinkhuis, H., Gibbs, S.J., Bralower, T.J., 2006. Extreme warming of mid-latitude coastal ocean during the Paleocene-Eocene Thermal Maximum: inferences from TEX86 and isotope data. Geology 34 (9):737–740. https://doi.org/10.1130/G22522.1.

Zachos, J.C., Dickens, G.R., Zeebe, R.E., 2008. An early Cenozoic perspective on greenhouse warming and carbon-cycle dynamics. Nature 451:279–283. https://doi.org/10.1038/nature.

Zeebe, R.E., 2012. History of seawater carbonate chemistry, atmospheric CO_2, and ocean acidification. Annual Review of Earth and Planetary Sciences 40:141–165. https://doi.org/10.1146/annurev-earth-042711-105521.

Zeebe, R.E., Zachos, J.C., Dickens, G.R., 2009. Carbon dioxide forcing alone insufficient to explain Palaeocene–Eocene Thermal Maximum warming. Nature Geoscience 2: 576–580. https://doi.org/10.1038/ngeo578.